

# Rotational Isomerism Involving Acetylene Carbon

Shinji Toyota\*

Department of Chemistry, Faculty of Science, Okayama University of Science, 1-1 Ridaicho, Kita-ku, Okayama 700-0005, Japan

Received February 22, 2010

## Contents

1. Introduction	5398
2. General Remarks	5399
2.1. Conformation about Acetylene Axis	5399
2.2. Acetylene and Related Linkers	5400
2.3. Methods of Study	5400
3. Rotational Isomerism of Fundamental Alkynes	5401
3.1. 2-Butyne (Extended Ethane)	5401
3.2. Diphenylethyne (Extended Biphenyl)	5401
3.3. 1,5-Hexadien-3-yne (Extended 1,3-Butadiene)	5402
4. Factors Influencing Rotational Isomerism	5402
4.1. Substituents at Propargylic Positions	5403
4.2. Substituents at sp Carbons	5404
4.3. Linker Length	5404
4.4. Conjugation	5404
4.5. Steric Effects	5405
4.6. Noncovalent Interactions	5405
4.7. Solvent Effects	5405
4.8. State of Sample	5406
4.9. Electronic Excited and Charged Species	5406
4.10. Miscellaneous Effects	5406
5. Strategic Control of Rotational Isomerism	5406
5.1. Restricted Rotation	5406
5.1.1. Acyclic Diarylethyne	5406
5.1.2. Acyclic Dialkylethyne	5407
5.1.3. Cyclic Alkylethyne	5408
5.1.4. Cyclic Arylethyne	5408
5.1.5. Metalated Alkynes	5411
5.2. Facilitated Rotation in the Solid State	5411
5.3. Folding of Acyclic Alkynes	5412
5.3.1. Helicates	5412
5.3.2. Molecular Hinges	5413
5.4. Tuning of Photophysical Properties	5414
5.4.1. Bis(phenylethynyl)anthracene Chromophores	5414
5.4.2. Porphyrin Chromophores	5414
6. Applications of Rotation about Acetylene Axis	5415
6.1. Molecular Vehicles	5415
6.2. Molecular Wires	5416
6.3. Molecular Scaffolds	5417
6.4. Molecular Recognition	5420
7. Conclusions and Perspectives	5420
8. Acknowledgments	5421
9. Note Added in Proof	5421
10. References	5421

## 1. Introduction

“Rotational isomerism” is one of the basic concepts in stereochemistry. It refers to isomerism that is due to the difference in spatial arrangement of atoms affording distinction between stereoisomers that can be interconverted by rotations about *formally single bonds*.<sup>1</sup> In principle, this concept can be extended to rotations about *any linear axes* involving more than one bond, with a typical example being the C—C≡C—C axis involving acetylene carbons. Eliel et al. published a comprehensive book on organic stereochemistry in 1994.<sup>2</sup> However, there was only *one short paragraph* on the rotational isomerism of triple bonded species. This could be attributed to the fact that the barriers to rotation were so low that studies of this topic were much less frequent than those of the ordinary rotational isomerism about single bonds, and phenomena related to their rotational isomerism were of little interest to organic chemists.

2-Butyne (**1**, dimethylacetylene) is the simplest alkyne whose rotational isomerism can be taken into consideration (Figure 1). This molecule is analogous to ethane (**2**) in terms of conformation and symmetry but differs in the axis moiety connecting the two methyl groups, if a rigid linear axis is assumed. The determination of the rotational barrier of 2-butyne is still a challenging subject in the field of spectroscopic chemistry. The energy changes during the rotation of one methyl group relative to the other are so small that special techniques and analyses are needed for quantitative determination. Another fundamental compound in the present topic is diphenylethyne (**3**, diphenylacetylene, tolane, abbreviated as DPE hereafter), which is analogous to biphenyl (**4**). Because the terminal benzene rings can electronically communicate with each other across the acetylene axis, this repeating unit is a fascinating tool for the construction of novel  $\pi$ -conjugated compounds in the fields of molecular switches and electronics.<sup>3,4</sup>

The structural modification that involves the insertion of a -C≡C- unit into single bonds is sometimes called “exploded”, as proposed by Houk and Scott et al.<sup>5</sup> Similarly, the exploded analogues are called “*carbo-mers*” of the parent compounds, as proposed by Maraval and Chauvin.<sup>6,7</sup> While these terms are used to indicate the insertion of C<sub>2</sub> units into all bonds in a strict sense, partial *carbo-mers* can be defined as compounds whose structures are modified at selected bonds only. Hence, 2-butyne and DPE are regarded as exploded compounds (or *carbo-mers*) of ethane and biphenyl, respectively. Despite the usefulness of these terms, the word “extended” will be used to indicate the structural change from X—Y to X—C≡C—Y in most cases and the elongation of a single bond axis with long linear linkers, for example polyynes or those containing 1,4-phenylene groups, in a broad sense.

\* E-mail: stoyo@chem.ous.ac.jp.



Shinji Toyota, born in 1964 in Japan, studied chemistry at The University of Tokyo. He received his Master's degree in 1988 there under the supervision of Professor Michinori Ōki and then became a research assistant at Okayama University of Science (OUS). After he received his Doctor's degree in 1992 with a thesis on dynamic NMR studies of organoboron compounds from The University of Tokyo, he was promoted to full professor in 2002. He stayed at University of California at San Diego as a visiting researcher in 1996–1997. He has been holding an additional position as the vice-president of OUS since 2008. He is interested in physical organic chemistry, supramolecular chemistry, and stereochemistry. Recently, he is engaged in research on the design and synthesis of novel arene–acetylene oligomers.

Recently, the acetylene axis has been extensively employed as a linker in the construction of various molecular scaffolds because it connects two moieties linearly at an interval of 4.1 Å with the least steric demand.<sup>8</sup> This function has been adopted in molecular machines and devices:<sup>9</sup> for example, wheels are connected to a body with acetylene linkers in molecular cars, where the acetylene axes work as freely rotating shafts (see section 6.1). The acetylene axis is often used as the axle part in molecular rotors to connect a rotor to a stator or two rotors.<sup>10</sup> In some alkynes, the rotation is no longer free for structural reasons, and this feature makes it possible to control conformational preference, even though the rotation occurs much more easily than that in nonextended systems. The remarkable progress in acetylene chemistry is due to the development of practical synthetic methods<sup>11,12</sup> involving metal-catalyzed coupling reactions, particularly Sonogashira coupling,<sup>13,14</sup> alkyne metathesis,<sup>15,16</sup> elimination reactions,<sup>17–20</sup> and rearrangements reactions, such as Fritsch–Buttenberg–Wiechell rearrangement<sup>21</sup> and Corey–Fuchs reaction,<sup>22</sup> but the synthetic aspect is beyond the scope of this review.

This review describes progress in rotational isomerism involving sp carbons in alkynes and the relationship between rotational isomers that differ in conformation about the acetylene axes or related linear axes, as an emerging area in stereochemistry. Section 2 provides general remarks essential for the consideration of rotational isomerism about the long

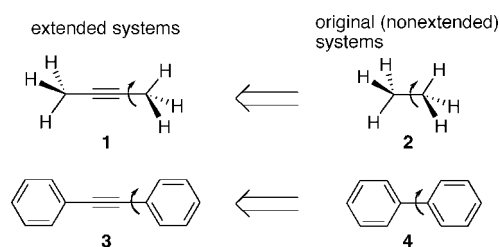


**Figure 1.** Conformation of ethane (2) and biphenyl (4) and their extended systems, 2-butyne (1) and diphenylethyne (3, DPE).

axes, including terminology, nomenclature, the structural features of various linear linkers, and the methods of study. In section 3, the conformational analysis of a few fundamental alkynes is explained to understand the basis of the rotational isomerism of acyclic alkynes and to compare their characteristics with those of nonextended systems. The rotational barriers are influenced by such factors as steric and electronic effects, which are classified in section 4 on the basis of the experimental and theoretical data of various alkynes. Sections 5 and 6 introduce recent examples of structurally or functionally fascinating alkynes in which rotational isomerism plays important roles. The strategic control of rotational barriers, namely, enhancing rotational barriers in solution and facilitating rotation in the solid state, is a challenging attempt to revise common knowledge in general organic chemistry. The regulation of the conformation of acyclic alkynes by molecular interactions and solvent effects is an emerging area aimed at realizing regularly shaped molecules, such as molecular helices. Recent applications of the rotational function to the molecular design of supramolecules and functional molecules are instructive to survey the scope and limitations of the role of acetylenes as a shaft or an axle<sup>23,24</sup> from structural and electronic viewpoints. As examples of such, molecular vehicles, one-, two-, and three-dimensional molecular architecture, and sensing molecules based on photophysical properties are selected, although not comprehensively, from relatively recent studies.

## 2. General Remarks

### 2.1. Conformation about Acetylene Axis

General conventions and concepts of the conformation about a single bond<sup>1,25</sup> are applicable to the conformation in an extended system, assuming that the acetylene axis is practically linear. An important difference is the length of the central axis connecting the two terminal groups, ca. 1.5 Å vs 4.1 Å, which leads to a considerable decrease in the effects of conformation on the energies and properties of alkynes. The conformation of alkynes is represented by such conventional methods as stereochemical formulas and Newman projections. Figure 2 shows examples of 3-hexyne (5), where the Newman projections are viewed along the three bonds (or four atoms) involving the central triple bond and the attaching two single bonds. Based on the torsion angles between two specified groups at both termini along the linear axis (called fiducial groups), one can define the conformation by the Klyne–Prelog nomenclature<sup>1,26</sup> as *antiperiplanar* (*ap*), *synclinal* (*sc*), and so on or by other conventional terms, *anti*, *gauche*, eclipsed, and staggered in obvious cases. When the axis is significantly bent from the linear geometry, the definition of torsion angles may be ambiguous. In such a

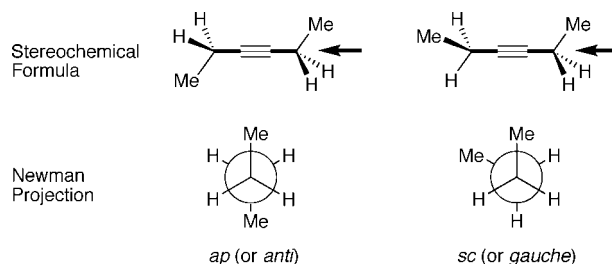


**Figure 2.** Representation of the conformation of 3-hexyne (5) along the acetylene axis. Only one form is shown for the *sc* conformation.

case, the conformation should be characterized by bond angles and torsion angles.

The rotational isomerism about an acetylene axis is fully characterized by the energy profile, i.e., the change in potential energy during the rotation by  $360^\circ$  as a function of the torsion angle, similarly to that about a single bond. In general, potential energy  $V$  is approximately expressed by a Fourier-type equation (eq 1):

$$V = \frac{1}{2}V_1(1 - \cos \theta) + \frac{1}{2}V_2(1 - \cos 2\theta) + \frac{1}{2}V_3(1 - \cos 3\theta) + \dots \quad (1)$$

where  $\theta$  is the torsion angle and  $V_n$  are the potential constants of respective terms.<sup>27</sup> The absolute values of the potential constants are usually very small for the acetylene system. The rotational barrier is defined as the energy barrier between two adjacent minima of the rotamers, and the population of rotamers reaching equilibrium is determined by the relative energies of the minima. The mode and periodicity of rotational energies are dependent on the hybridization and substitution patterns of the terminal groups. The extended biphenyl, ethane, and toluene, namely, DPE, 2-butyne, and 1-phenyl-1-propyne, respectively, should possess 2-, 3-, and 6-fold potential curves, respectively. For example, the 3-fold potential is expressed by the above equation when  $V_1 = V_2 = 0$  and  $V_3 \neq 0$ .

## 2.2. Acetylene and Related Linkers

This review treats not only the ethynylene (monoacetylene) linker but also various linear linkers involving acetylene units. The length of a linear linker greatly influences the interactions between the terminal groups. The distances between the terminal carbon atoms in  $\text{C}\equiv\text{C}\text{--}\text{C}$  and  $\text{C}\equiv\text{C}\text{--}\text{C}\equiv\text{C}\text{--}\text{C}$  units are 4.2 Å and 6.8 Å, respectively, based on simple molecular mechanics (MM) calculations (Figure 3). In general, the length of polyynes linkers is a function of the number of triple bonds. *p*-Phenylene and related arylene groups (1,4-naphthylene and 9,10-anthrylene) are occasionally incorporated into the linear axis, if they are considered to be part of the linear axis. An additional *p*-phenylene unit lengthens the axis by approximately 4.3 Å. The length of linear linkers  $l$  consisting of  $x$  triple bond units and  $y$  *p*-phenylene units is approximately expressed in the equation in Figure 3, although the values are somewhat influenced by the order of repeating units and the hybridization of terminal groups.

Although alkynic carbons are assumed to be linear in the above discussion, the acetylene linkers are not as rigid in real molecules as one might expect for simple molecular models. Small deviations (ca.  $10^\circ$ ) from the linear geometry require small energies and are often observed for alkynic carbons in ordinary alkynes and polyynes. In some cyclic or strained alkynes, the bond angles can be as small as  $160^\circ$  or even smaller.<sup>28–31</sup> The bending deformation at each

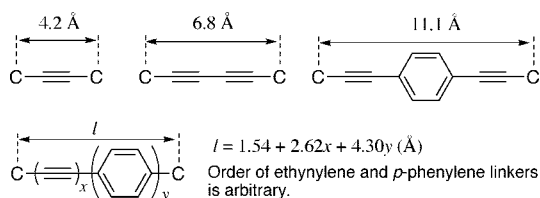


**Figure 3.** Typical linear linkers involving acetylene units and their linker lengths.

alkynic carbon results in a nonlinear  $\text{C}\text{--}\text{C}\equiv\text{C}\text{--}\text{C}$  linker, typically possessing a zigzag shape and a bow shape, as characterized by the torsion angle along the chain. For polyynes derivatives, a small deformation at each alkynic carbon leads to a remarkable curvature.<sup>32,33</sup> These deformations can be more significant in the transition state than in the original state during the rotation about the axis. Hence, the steric interactions between the terminal groups can be relieved to some extent by the flexibility of linker moieties in the transition state, resulting in the difficulty of barrier enhancement by the steric effects.

## 2.3. Methods of Study

Rotational isomerism involving acetylene carbons has been studied by experimental and theoretical methods conventionally used for conformational analysis.<sup>34</sup> For ordinary alkynes with very low barriers, the rotational barriers can be determined by spectroscopic (microwave or IR) or electron diffraction measurements. However, the determination of pure rotational barriers is not easy because of the association with vibrations and other rotations.<sup>27</sup> To overcome these limitations, modern and special spectroscopic techniques have been developed to observe such large-amplitude dynamics as those mentioned in the next section. NMR and X-ray spectroscopy are important methods for the conformational and structural analyses of alkynes. When the rotation is considerably restricted down to the NMR time scale, the dynamic process can be observed as line shape changes in the NMR signals. The dynamic NMR method and related techniques afford kinetic information on conformational exchanges.<sup>35</sup> Occasionally, long-range spin–spin coupling is observed between proton nuclei across an acetylene moiety. The coupling constants depend on the rates of rotation about the axis: for example, the rotational barrier was estimated to be 6 kJ/mol for phenylpropynal ( $\text{PhC}\equiv\text{CCHO}$ ) from the  $^8J_{\text{HH}}$  value between formyl and *p*-phenyl protons.<sup>36</sup> Density functional theory (DFT) calculations suggested that Karplus-type equations were obtained in the coupling constant between terminal methyl protons in 2-butyne ( $\text{H}\text{--}\text{C}\text{--}\text{C}\equiv\text{C}\text{--}\text{C}\text{--}\text{H}$ ) and longer analogues.<sup>37</sup> For 2,4-hexadiyne, the calculated coupling constants between the terminal methyl protons ( $^7J_{\text{HH}}$ ) change in the range of 0–3.2 Hz during the internal rotation by  $180^\circ$ , even though the protons are ca. 7.5 Å apart. Such relationships are helpful to predict the conformations of alkynes with protons at both propargylic positions ( $\text{sp}^3$  carbons next to the alkynyl group). X-ray structural analyses give direct information of the molecular structures in crystals. Structural features affected by conformation and strain can be readily discussed on the basis of the observed structural parameters.

Computational chemistry, such as MM, MO (semiempirical or ab initio), and DFT methods, has greatly contributed to progress in the conformational studies of alkynes, especially when experimental approaches are impossible or limited. Structural optimization should be carried out under strictly controlled conditions to obtain accurate structures at energy minima or maxima because of the very small energy changes during the rotation about the acetylene axis. Calculations at high levels tend to give reliable rotational barriers, as exemplified by the calculations of DPE and 2-butyne.

Rotational barriers are represented by various energy units according to the conventions of each method of study, preferably in  $\text{cm}^{-1}$  or eV for spectroscopic measurements



and in H (Hartree) for theoretical calculations. The unit of kJ/mol (or J/mol) will be used throughout this review. If necessary, the following equations may be applied for the unit conversion:  $1 \text{ kJ/mol} = 83.59 \text{ cm}^{-1} = 1.036 \times 10^{-2} \text{ eV} = 3.809 \times 10^{-4} \text{ H (Hartree)}$ .

### 3. Rotational Isomerism of Fundamental Alkynes

The rotational isomerism of three fundamental alkynes is described in this section: 2-butyne (**1**) with two methyl groups ( $\text{sp}^3$  substituents) at both ends, DPE (**3**) with two phenyl groups (aromatic  $\text{sp}^2$  substituents), and 1,5-hexadiene-3-yne (**6**) with vinyl groups (alkenic  $\text{sp}^2$  substituents), because several experimental and theoretical data have been accumulated for them (Figure 4). These data are helpful to monitor the progress in this research area and learn the conformational features of other alkynes.

#### 3.1. 2-Butyne (Extended Ethane)

As an example of large-amplitude motion, the internal rotation of 2-butyne (**1**) has been a subject of interest to many chemists for a long time. The rotational barrier of 2-butyne is much lower than that of DPE because of the absence of  $\pi$  conjugation. The energy profile is expected to be 3-fold, approximately represented by  $V = \frac{1}{2}V_3(1 - \cos 3\theta)$ , where the absolute value of  $V_3$  corresponds to the rotational barrier. The experimental and theoretical rotational barriers of 2-butyne are compiled in Table 1.

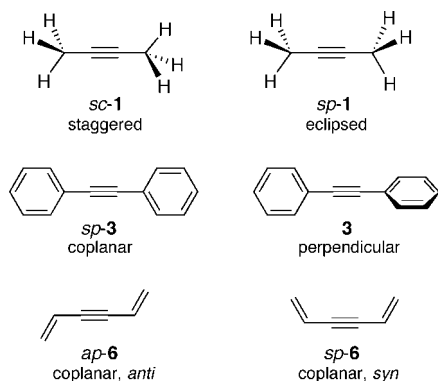


**Figure 4.** Typical conformations of fundamental alkynes, 2-butyne (**1**), DPE (**3**), and 1,5-hexadiene-3-yne (**6**).

**Table 1. Calculated and Experimental Rotational Barriers of 2-Butyne (1)**

method	barrier (J/mol)	ref
Experimental		
IR	<420	44
far-IR	<420	45
IR	<48	46
microwave spectra	67 <sup>a</sup>	47
IR	61	48
IR	76	49
Calculated <sup>b</sup>		
HF/STO-3G	25 <sup>c</sup>	51
HF/STO-4G	21 <sup>c</sup>	51
HF/4-31G	31	52
HF/4-31G	30	53
HF/6-311++G(3df, 3p)	63	54
MP2/6-311++G(3df, 3p)	56	54
B3LYP/6-311++G(3df, 3p)	74	54

<sup>a</sup> Determined for 2-butyne-1,1,1- $d_3$ . <sup>b</sup> The eclipsed form is the energy minimum unless otherwise stated. <sup>c</sup> The staggered form is the energy minimum.

Early studies by calorimetric measurements,<sup>38,39</sup> spectroscopic measurements,<sup>40</sup> and theoretical approaches<sup>41-43</sup> predicted no or negligibly low rotational barriers. Although some spectroscopic measurements proved the presence of the barrier later, only the upper limits were reported because of experimental limitations for the determination of very low potentials.<sup>44-46</sup> The first reliable experimental barrier, 67 J/mol, was reported by Nakagawa et al. in 1984 by microwave spectroscopy of partially deuterated 2-butyne.<sup>47</sup> Modern high-resolution IR measurements gave comparable values (61 and 76 J/mol) by analyzing  $\text{CH}_3$  rocking and C-H stretching bands, respectively.<sup>48,49</sup> However, these spectroscopic data cannot answer the question of whether the staggered or eclipsed form is more stable. The molecular structure of 2-butyne- $d_6$  was determined by neutron diffraction of the solid at 5 K.<sup>50</sup> In the refined structure, the two methyl- $d_3$  groups staggered each other along the linear acetylene axis.

Theoretical calculations of 2-butyne were performed by various methods. The eclipsed and staggered forms were obtained as the energy minimum and maximum structures, respectively, except for a few earlier results. The energy differences between the two conformations were underestimated (20–30 J/mol) by Hartree–Fock (HF) calculations with minimal or 4-31G basis sets.<sup>51,52</sup> The experimental values were reasonably reproduced by using basis sets with sufficient diffusion and polarization functions.<sup>53,54</sup> The effects of the electron correlation are small, as revealed by the calculated barriers by Møller–Plesset (MP) and B3LYP theories.<sup>54</sup> The rotational barrier was too low to detect by MM calculations with the MM3 force field.<sup>55</sup> The established barriers are ca. 1/200 of that of ethane (12 kJ/mol).<sup>25,56</sup> The interactions between the methyl groups are considerably weakened by the insertion of a triple bond.

#### 3.2. Diphenylethyne (Extended Biphenyl)

This compound is best studied among the alkyne derivatives as a model of diarylethyne. A DPE molecule principally has one degree of freedom, namely, rotation about the acetylene axis, and its conformation is specified by the dihedral angle ( $\theta_1$ ) between the two terminal phenyl groups (Figure 5). The energy profile is expected to be a 2-fold curve as a function of  $\theta_1$ , approximated to be  $V = \frac{1}{2}V_2(1 - \cos 2\theta_1)$ . There are several X-ray structures of DPE and its inclusion compounds, and at least nine polymorphic forms have been reported for the guest-free crystals, where the dihedral angles are completely or nearly  $0^\circ$ .<sup>57-60</sup> A perfectly planar structure is shown in Figure 6.<sup>57</sup> The distance between the proximate hydrogen atoms in different phenyl rings is 4.4 Å, being apparently longer than the sum of the van der Waals radii.

The experimental and calculated rotational barriers of DPE are compiled in Table 2. It was difficult to determine the rotational barrier at the ground state by ordinary spectroscopic methods. In 1984, the first reliable experimental rotational barrier was determined by single vibronic level fluorescence spectroscopy in a supersonic free jet.<sup>61</sup> The coplanar conformation ( $\theta_1 = 0^\circ$ ) is more stable by 2.4 kJ/mol than the perpendicular conformation ( $\theta_1 = 90^\circ$ ), and this height corresponds to the 15th vibrational quantum state (Figure 5). A similar value was also obtained by electron diffraction on the basis of a dynamic model<sup>58</sup> and by an adsorption experiment on graphite.<sup>62</sup>

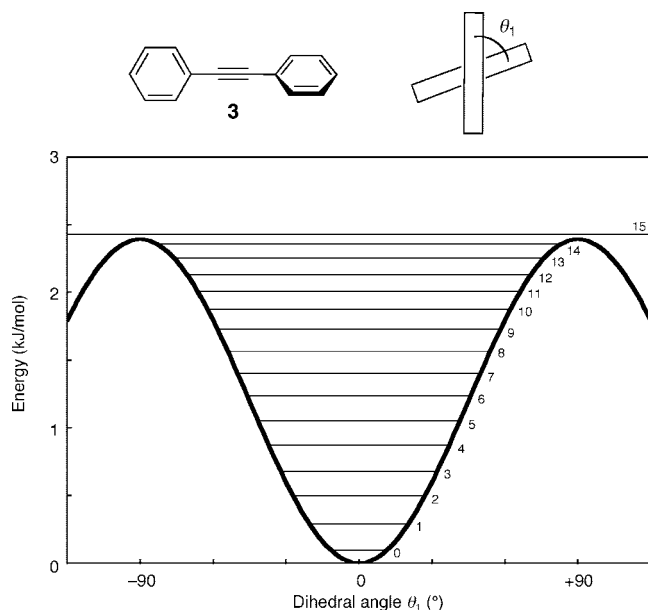


**Figure 5.** Potential curve of torsional motion of DPE (**3**) determined by fluorescence spectroscopy. Horizontal lines indicate vibrational levels with quantum numbers. Adapted with permission from ref 61. Copyright 1984 American Chemical Society.

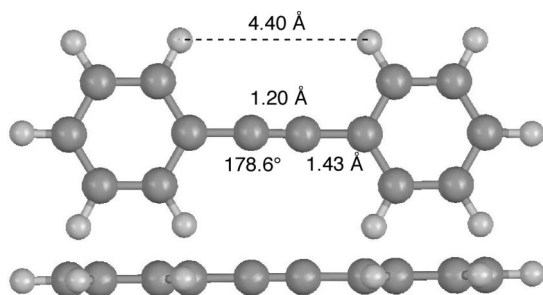


**Figure 6.** Two views of a typical X-ray structure of DPE with selected structural parameters (one of the independent molecules in the X-ray data in ref 57).

**Table 2.** Calculated and Experimental Rotational Barriers of DPE (**3**)

method	barrier (kJ/mol)	stable conformation	ref
Experimental			
fluorescence	2.4	coplanar	61
electron diffraction	2.5	coplanar <sup>a</sup>	58
adsorption	2.5	coplanar	62
Calculated			
CNDO	2.9	perpendicular	63
INDO	1.7	perpendicular	63
CNDO/2	2.7	perpendicular	59
AM1	0.90	coplanar	64
HF/6-31G*	1.8	coplanar	64
MP2/6-311G**	2.7	coplanar	66
B3PW91/6-311G**	3.6	coplanar	67
B3LYP/6-311+G**	3.3	coplanar	68
B3LYP/6-31G**//AM1	4.1 <sup>b</sup>	coplanar	69

<sup>a</sup> The stable conformation depends on the model used for the refinement. <sup>b</sup> The transition state is a nearly bisected conformation rather than the bisected conformation, which is a local energy minimum.

Earlier calculations by semiempirical methods gave barriers of 2–3 kJ/mol, where the bisected conformation was the global minimum, contrary to the experimental result.<sup>56,63</sup> The preference for the coplanar conformation was predicted by AM1 and HF calculations, regardless of the underestimation of the barrier height.<sup>64,65</sup> The high level calculations

based on the second-order MP (MP2) perturbation theory and DFT with hybrid-type functionals (B3PW91 and B3LYP) gave reasonable results.<sup>66–69</sup> The stability of the coplanar conformation can be rationalized by the full conjugation of the  $\pi$  electron systems of the two phenyl groups through the C $\equiv$ C bond. More about the roles of conjugation will be mentioned in section 4.4.

The thus obtained energy mode and magnitude are different from those of biphenyl, where the dihedral angles between the two phenyl groups are 44° in the global minimum and 0° and 90° in the transition states.<sup>70,71</sup> The rotational barriers between the staggered conformations across the two transition states are both predicted to be ca. 8 kJ/mol. The energy maximum in the coplanar conformation in biphenyl is attributed to the increased steric hindrance between the *o*-hydrogen atoms at proximate positions (interatomic distance 2.1 Å). It should be noted that DPE still has a significant barrier that is as high as one-third of the barrier of biphenyl.

### 3.3. 1,5-Hexadien-3-yne (Extended 1,3-Butadiene)

1,5-Hexadien-3-yne (**6**: divinylethyne) has two kinds of coplanar conformations, *sp* (*s-cis*) and *ap* (*s-trans*), in addition to other nonplanar conformations. As the two eclipsed conformations have different energies, the potential energy should contain a 1-fold term. The electron diffraction data of **6** at 20 °C are explained by a free rotation model rather than a model of both *sp* and *ap* forms or either of them: the rotational barrier is too low to detect by this method.<sup>72</sup> The IR spectra are consistent with the symmetry of the *ap* conformation.<sup>73</sup> The theoretical calculations gave two energy minima at the two coplanar conformations of comparable stabilities and one energy maximum at the nearly perpendicular conformation. The energies required for the interconversion from the *sp* form to the *ap* form are 0.85 kJ/mol (AM1), 2.0 kJ/mol (HF/6-31G\*), and 2.2 kJ/mol (MP2/6-31G\*).<sup>74–76</sup> As for 1,3-butadiene, the *sp* form suffers from steric interactions and is less stable by 12 kJ/mol than the *ap* form.<sup>77–79</sup> The rotational barrier of the *ap* to *sc* process was determined to be ca. 30 kJ/mol by experimental and theoretical methods.<sup>77</sup>

The conformational features of the three fundamental alkynes and their nonextended analogues are compiled in Table 3.

## 4. Factors Influencing Rotational Isomerism

The rotational barriers and populations of alkyne conformers are influenced by various factors, such as steric and electronic effects, as discussed in general kinetic and thermodynamic studies.<sup>80,81</sup> Other intermolecular and intramolecular interactions, such as hydrogen bond, solvation, electronic states, state of sample, and external stimulus, are possible factors affecting the rotational isomerism. The through-bond and through-space interactions between the two terminal groups in alkynes are usually much weaker than those in the corresponding nonextended analogues, as seen for the three fundamental alkynes in the last section. Therefore, the extent of these effects decreases sharply with the extension of the central axis unless through-space interactions operate effectively. The characteristics of each factor or mode of substitution are described below, although it is not always easy to separate overall effects into respective factors.

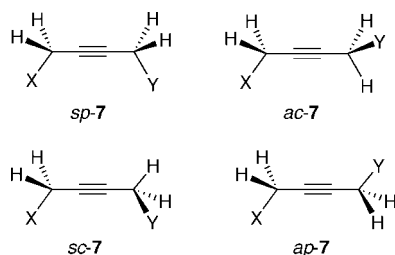
**Table 3. Conformational Features of Extended and Original Compounds of Three Fundamental Systems**

system (mode of conformational energy)	ethane system (3-fold)		biphenyl system (2-fold)		1,3-butadiene system (1-fold)	
	2-butyne	ethane	DPE	biphenyl	1,5-hexadiene-3-yne	1,3-butadiene
stable conformation	eclipsed ( <i>sp</i> )	staggered ( <i>sc</i> )	coplanar ( <i>sp</i> )	staggered ( <i>sc</i> )	coplanar ( <i>sp</i> and <i>ap</i> )	coplanar ( <i>ap</i> )
conformation in transition state	staggered ( <i>sc</i> )	eclipsed ( <i>sp</i> )	perpendicular	coplanar ( <i>sp</i> ) and perpendicular	perpendicular	<i>ac</i>
rotational barrier (kJ/mol)	0.07	12	3	8	2 ( <i>ap</i> → <i>sp</i> )	ca. 30 ( <i>ap</i> → <i>sp</i> )

#### 4.1. Substituents at Propargylic Positions

Conformational analyses of various substituted 2-butyne **7** (Figure 7) were carried out by HF calculations.<sup>53</sup> The data in Table 4 suggest that the conformational stabilities and the rotational barriers are dependent on the nature and combination of substituents at the propargylic positions. 2-Pentyne ( $X = \text{CH}_3$ ,  $Y = \text{H}$ : extended propane) and 3-hexyne ( $X = \text{CH}_3$ ,  $Y = \text{CH}_3$ : extended butane) prefer to take the eclipsed conformation, where the two methyl groups are *ac* in the latter. The rotational barriers of these alkynes (50–80 J/mol) are comparable to that of 2-butyne. In contrast, microwave studies revealed that the two substituents were eclipsed; that is, they had the *sp* conformation in 3-hexyne and 3-heptyne in the gas phase.<sup>82,83</sup> The preference for the eclipsed conformation means that the hyperconjugation that stabilizes the staggered conformation, as discussed in the rotational barrier of ethane by Goodman et al.,<sup>56</sup> is negligible in the extended system.

The presence of one electronegative or one electropositive substituent at the propargylic position results in small effects on the energy profile. The observed barrier to internal rotation was 0.12 kJ/mol for 1-chloro-2-butyne ( $X = \text{Cl}$ ,  $Y = \text{H}$ ).<sup>84,85</sup> On the other hand, the presence of two electronegative or two electropositive substituents at the propargylic positions apparently increases the rotational barriers and changes the shapes of the potential curves. For 1,4-difluoro, dichloro, and dilithio derivatives ( $X = Y = \text{F}$ ,  $\text{Cl}$ , or  $\text{Li}$ ), the two substituents are *ac* in the energy minimum conformation. As for 1,4-dichloro-2-butyne, the torsion angle between the two Cl atoms along the acetylene axis is  $120^\circ$  in the global minimum, and

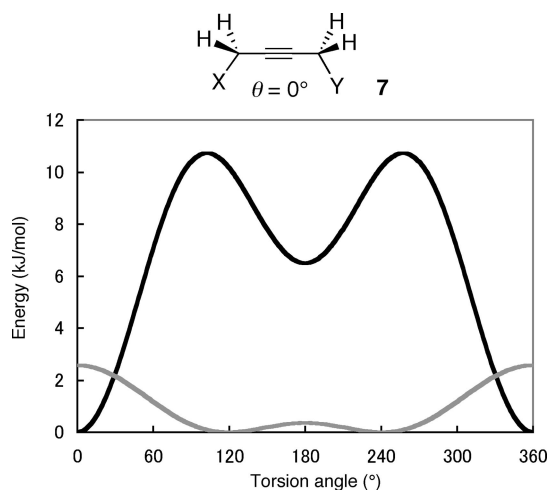
**Figure 7.** Conformations of 1,4-disubstituted 2-butyne (**7**).**Table 4. Calculated Results of the Conformation of 1,4-Substituted 2-Butynes (**7**) ( $X-\text{CH}_2\text{C}\equiv\text{CCH}_2-\text{Y}$ )**

substituent X, Y		method	stable conformation (deg) <sup>a</sup>	barrier (kJ/mol) <sup>b</sup>	ref
H	H	HF/4-31G	0	0.03	53
H	CH <sub>3</sub>	HF/4-31G	0	0.05	53
CH <sub>3</sub>	CH <sub>3</sub>	HF/4-31G	120	0.03 ( <i>ap</i> ), 0.08 ( <i>sp</i> )	53
H	F	HF/4-31G	0	0.03	53
H	Li	HF/4-31G	0	0.03	53
F	F	HF/4-31G	103.7	2.1 ( <i>ap</i> ), 5.3 ( <i>sp</i> )	53
Li	Li	HF/4-31G	113.9	2.7 ( <i>ap</i> ), 15.8 ( <i>sp</i> )	53
Li	F	HF/4-31G	0	10.7	53
Cl	Cl	HF/6-31G*	120	0.35 ( <i>ap</i> ), 2.6 ( <i>sp</i> )	76

<sup>a</sup> Torsion angles between X and Y along the acetylene axis. <sup>b</sup> Barriers across *ap* and *sp* conformations when two values are given.

the rotational barriers across the *ap* and *sp* conformations are 0.35 and 2.6 kJ/mol, respectively (Figure 8).<sup>76</sup> In contrast, the presence of one electronegative substituent and one electropositive substituent ( $X = \text{F}$ ,  $Y = \text{Li}$ ) stabilizes the *sp* conformation via hyperconjugation between C–Li and C–F bonds across the triple bond.<sup>53</sup> The rotational barrier from the stable *sp* to the less stable *ap* conformer was calculated to be 11 kJ/mol for 1-fluoro-4-lithio-2-butyne.

The conformations of other substituted 2-butyne were studied by experimental and theoretical methods. Microwave spectroscopy revealed that 6-methyl-3-heptyne existed as a mixture of two conformers, where the two terminal substituents, Me and *i*-Pr groups, were eclipsed along the linear axis.<sup>86</sup> The rotational barrier of the methyl group in 2-butyne-1-ol was determined by microwave analysis to be 83 J/mol, although the stable conformation about the acetylene axis was not specified.<sup>87</sup> The rotational barrier of 1,1,1-trifluoro-2-butyne was too low to measure by microwave spectroscopy, being consistent with the result of early MO calculations (16 J/mol).<sup>88</sup>

**Figure 8.** Energy profile of the conformation of 1,4-disubstituted 2-butyne (**7**): gray, 1,4-dichloro-2-butyne ( $X = Y = \text{Cl}$ ) at HF/6-31G\*; black, 1-fluoro-4-lithio-2-butyne ( $X = \text{F}$ ,  $Y = \text{Li}$ ) at HF/4-31G. Torsion angles are defined by the arrangement of substituents X and Y.

## 4.2. Substituents at $sp$ Carbons

The direct substitution of nonalkyl substituents, particularly heteroatom substituents, at  $sp$  carbons could result in large effects on the conformational energy profile compared with the substitution at the propargylic positions. The calculated data of variously substituted alkynes  $X-C\equiv C-Y$  are compiled in Table 5. In general, a coplanar conformation is stabilized by a donor substituent and an acceptor substituent at each terminal. DFT calculations predicted that the coplanar conformation was more stable by 24 kJ/mol than the perpendicular one for 3-aminopropynal (**8**), while the perpendicular conformations were more stable for diamino **9** and diformyl **10** derivatives (Figure 9).<sup>89</sup> The difference in the stable conformation was deduced by the orbital phase theory. Similarly, the preference for the coplanar conformation was also suggested for alkyne **11** with  $NH_2$  and  $BH_2$  groups because of the contribution of charge-separated resonance structures, as depicted in Figure 9.<sup>90</sup> Alkynes with two oxygen substituents at both ends prefer to take the perpendicular conformations, similarly to the diamino and diformyl derivatives.<sup>74</sup> A 3-fold barrier to internal rotation was confirmed by microwave spectroscopy of 2-butyne fluoride ( $CH_3-C\equiv C-COF$ ), where the  $V_3$  term was estimated to be 26 kJ/mol.<sup>91</sup>

The conformations of some alkynes with third-row element substituents have also been reported. The calculations suggested that the conformational feature of 1,2-dimercaptoethyne (**13**) was similar to that of the oxygen analogue **12**, although the former tended to enhance the rotational barriers due to the high polarizability of S atoms.<sup>74</sup> The rotational barrier of 1-propynylsilane was determined by millimeter-wave spectroscopy to be 45 J/mol as the  $V_3$  term.<sup>92</sup> The calculated rotational barrier of bis(trimethylsilyl)ethyne is 40 J/mol at the MP2/6-311G\*\* level, where the staggered conformation of the  $D_{3d}$  symmetry is slightly more stable than the eclipsed one.<sup>93</sup> The barrier heights of these silyl-substituted alkynes are comparable to that of 2-butyne. The conformations of hypervalent silicon derivatives,  $R-C\equiv C-SF_4^-$ , were also calculated by the DFT method, and the stable conformation was determined by the nature of substituents R through orbital interactions between the terminal groups.<sup>89</sup>

## 4.3. Linker Length

As for diyne and longer polyene linkers, energy changes during the rotation of the terminal groups rapidly decrease as the lengths of the linear linkers increase. This trend is supported by theoretical calculations of the aminoaldehyde and aminoborane derivatives, as shown in Table 5.<sup>89,90</sup> For

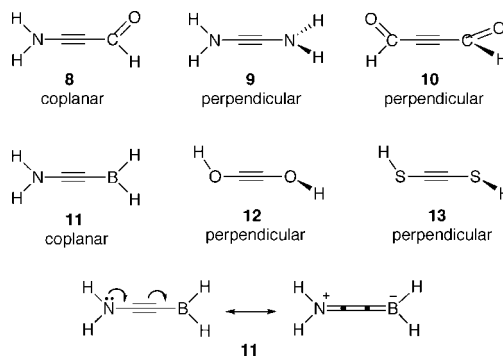


**Figure 9.** Stable conformations of alkynes with various substituents at  $sp$  carbons.

each series of compounds, the insertion of an extra  $-C\equiv C-$  decreases the barriers by 40–70%. A similar trend should be found in further extended analogues of 2-butyne and DPE, although reliable experimental and theoretical data of such compounds are quite limited.<sup>94–96</sup> The vibrational spectra of some diynes were satisfactorily analyzed on the assumption of  $D_{3d}$  symmetry for 2,4-hexadiyne and 2,2,7,7-tetramethyl-3,5-octadiyne and  $D_{2h}$  symmetry for 1,4-diphenylbutadiyne, although the vibration frequencies relating to conformational motion were difficult to assign.<sup>97–99</sup> This structural feature of diyne and longer linkers, namely, practically free rotation, has been utilized in the design of functional molecules and macrocyclic compounds, as mentioned later.

## 4.4. Conjugation

The roles of conjugation have been discussed above in terms of the preference for the coplanar conformation of DPE and related compounds, and additional examples are described here. According to a simple model, the overlap of p orbitals of the two-terminal  $\pi$  systems with the same set of alkyne p orbitals leads to the coplanar conformation, while that with a different set of p orbitals leads to the perpendicular conformation.<sup>63</sup> The low barrier of DPE means that the difference in conjugation in the two modes is hardly of major importance in determining the conformation about the acetylene axis.<sup>58</sup> The bond order of the formally single bond is 1.18 in the X-ray structure of coplanar DPE, and this value suggests a relatively low degree of conjugation.<sup>59</sup> Charge density analysis of the X-ray diffraction data revealed that the electron density around the acetylene linker in DPE was apparently noncylindrical, with a small ellipticity indicating the extended conjugation.<sup>57</sup> As shown in the orbital plots in Figure 10, the orbital of coplanar DPE spreads over the molecule at the HOMO level due to effective conjugation, whereas the other p orbitals of the alkyne are nearly localized

**Table 5.** Calculated Data of the Conformations of Various Alkynes and Polyynes [ $X-(C\equiv C)_n-Y$ ]

substituents X, Y	$n$	method	stable conformation (deg) <sup>a</sup>	barrier (kJ/mol)	ref
NH <sub>2</sub> CHO	1	B3LYP/6-31+G*	0	24.4	89
NH <sub>2</sub> CHO	2	B3LYP/6-31+G*	0	12.5	89
NH <sub>2</sub> CHO	3	B3LYP/6-31+G*	0	7.4	89
CHO CHO	1	B3LYP/6-31+G*	90	4.0	89
NH <sub>2</sub> NH <sub>2</sub>	1	B3LYP/6-31+G*	90	21.7	89
NH <sub>2</sub> BH <sub>2</sub>	1	STO-3G	0	25.1	90
NH <sub>2</sub> BH <sub>2</sub>	2	STO-3G	0	8.0	90
NH <sub>2</sub> BH <sub>2</sub>	3	STO-3G	0	2.8	90
OH OH	1	HF/6-31G*	90	7.7 (sp), 5.3 (ap)	74
OCH <sub>3</sub> OCH <sub>3</sub>	1	HF/6-31G	102	7.7 (sp), 3.6 (ap)	74
SH SH	1	HF/6-31G	90	13.8 (sp), 13.4 (ap)	74

<sup>a</sup> Torsion angles between fiducial groups along the acetylene axis. See Figure 9.



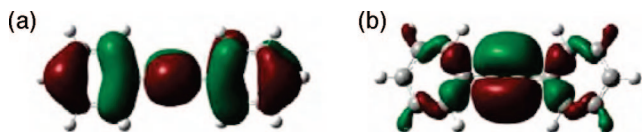


**Figure 10.** HOMO (a) and HOMO-3 (b) orbital plots of coplanar DPE (**2**) calculated at B3LYP/6-31G(d). Reprinted with permission from ref 57. Copyright 2006 American Chemical Society.

at the *sp* carbons at a lower energy level. The degree of conjugation can be evaluated from the electronic spectra. Spectroscopic measurements of some conformationally fixed DPE derivatives showed that the UV–vis absorption bands were blue-shifted as the two phenyl groups were twisted from the coplanar conformation.<sup>69</sup>

#### 4.5. Steric Effects

The substituents at both ends of the acetylene moiety are so far from each other that the steric interactions between the two moieties are expected to be minimal. If the steric interactions seem to be present in a rigid molecular model, they can be relieved by the bending deformation at *sp* carbons and the attaching carbon atoms to avoid excess steric hindrance in the transition state. Regardless of these structural situations, bulky substituents can retard rotation due to destabilization of the transition state by steric hindrance. Energy profiles of the conformational changes in perhalogenated DPE derivatives **14** (*X* = F, Cl, or Br) were determined by MM calculations (Figure 11).<sup>100</sup> In the global minimum, the dihedral angles between the two phenyl groups are 0, 25, and 55° for **14a–c**, respectively. These values indicate that the coplanar conformation is obviously destabilized by the nonbonding contact in Br compound **14c**. The rotational barrier between the global minimum staggered conformations across the coplanar conformation was calculated to be 20 kJ/mol in **14c**. A similar substituent effect was also observed in the 1,3-butadiene system. In perchloro-1,5-hexadien-3-yne (**15**), the *sp* form is not an energy minimum anymore because of the steric effect, and the rotational barrier from the global minimum *sc* form ( $\theta = \text{ca. } 35^\circ$ ) to the local minimum *ap* form is ca. 8 kJ/mol (cf. 2 kJ/mol for 1,5-hexadien-3-yne) according to electron diffraction and MM studies.<sup>72</sup> Further examples of hindered rotation by bulky substituents will be introduced in section 5.1.

When two rotors are oriented at an appropriate distance and angle, the rotation of one rotor may be correlated with that of the other rotor, as observed for di(9-triptycyl)methane and ether derivatives.<sup>101</sup> It seems to be difficult to realize such molecular gears with acetylene linkers because the

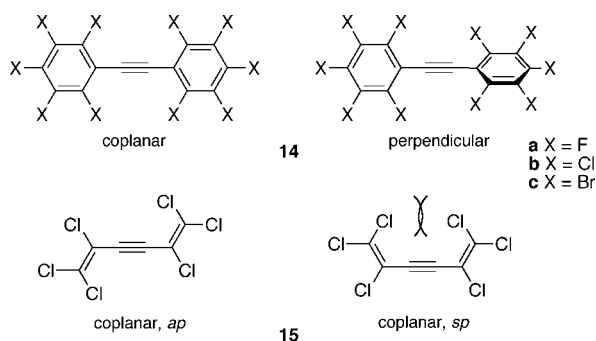


**Figure 11.** Conformations of halogenated extended biphenyls **14** and extended 1,3-butadiene **15**.

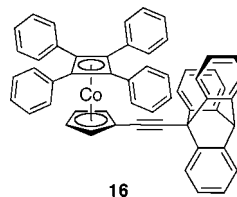


**Figure 12.** Gear-type molecule having a triptycene rotor and a metallocene rotor.

flexibility of the axis moieties leads to gear slippage. Compound **16**, having a triptycene (three-toothed) rotor and a metallocene (four-toothed) rotor, was proposed as a molecular gear, although there was no conclusive evidence of the correlated rotation (Figure 12).<sup>102</sup>

#### 4.6. Noncovalent Interactions

Attractive interactions, such as a hydrogen bond, can play significant roles in fixing the conformation or enhancing the rotational barrier of alkyne derivatives. Compound **17** with functional groups at the 2 and 2' positions prefers to take *sp* conformation **17a** because of the stabilization by the intramolecular hydrogen bond between the ester and amide moieties (Figure 13).<sup>103,104</sup> This coplanar conformation is more stable than coplanar *ap* form **17b** by 24 kJ/mol, and the barrier to rotation from **17a** to **17b** is 30 kJ/mol, 12 times that of DPE, according to the calculation at the B3LYP/6-31G(d,p) level. The conformation of a similar derivative **18** is also defined by an intramolecular hydrogen bond.<sup>105</sup> Similarly, C–H···O, C–H··· $\pi$ , and  $\pi$ ··· $\pi$  interactions and metal coordination can control the rotational barrier and the rotamer population. Some concrete examples are given in the following divisions.

#### 4.7. Solvent Effects

Solvent effects on the conformation of alkyne derivatives are similarly considered to general chemical processes in terms of polarity, protic/aprotic property, solvation, and so on.<sup>106</sup> However, solvent effects are very difficult to observe by experimental methods because the energy differences in kinetics and thermodynamics are very small for ordinary alkynes. Nevertheless, solvophobic (or solvophilic) effects play dominant roles in controlling the conformation of some oligomeric alkynes bearing hydrophilic side chains. Examples of helical foldamers based on solvophobic effects are introduced in section 5.3.1.<sup>107</sup> The rotational barrier of DPE in a liquid crystal solvent was determined by the theoretical analysis of spin coupling constants.<sup>108,109</sup> The calculated barrier of 3.6 kJ/mol is higher by ca. 1 kJ/mol than the

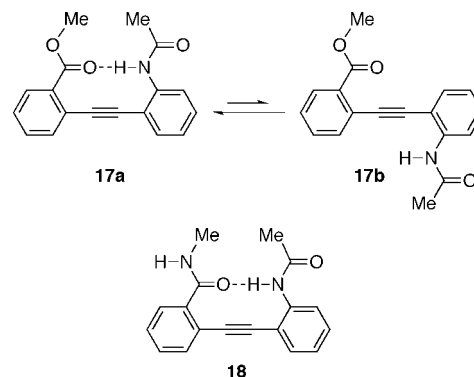


**Figure 13.** DPE derivatives bearing hydrogen bond sites.



experimental value in the gas phase (Table 2) because the coplanar conformation is stabilized by the liquid crystal solvent.

#### 4.8. State of Sample

In most cases, experimental measurements to determine the rotational barriers are carried out in the gas and liquid states or in solution. The mobility of molecules is considerably restricted in the solid state compared with the above conditions because of the strong intermolecular interactions. However, the motion is not completely frozen in the solid state. A sample of crystalline 2-butyne was investigated by  $^1\text{H}$  NMR at low temperature, and the analysis of  $T_1$  values gave a barrier of 3.5 kJ/mol.<sup>110</sup> Neutron scattering measurement at 4.5 K gave a comparable barrier of 4 kJ/mol.<sup>111,112</sup> On the basis of the X-ray crystal structure of DPE, the rotational barrier (4.9 kJ/mol) was calculated with a model of semirigid molecules.<sup>113</sup> As far as we know, there is no report of the internal rotation in 2,4-hexadiyne in the fluid state. However, its rotational barrier was determined by neutron scattering measurement at 4 K in the solid state to be 5.5 kJ/mol.<sup>114</sup>

The rotation of phenyl groups is considerably restricted in the solid state because of intermolecular contacts in the packing. In an Ar matrix at 5 K, DPE molecules are frozen into several conformations to give many bands in the electronic spectra.<sup>115</sup> This experimental result was supported by molecular dynamics (MD) calculations, which also simulated the relaxation of the frozen conformers into different conformers.<sup>116</sup> A tactical molecular design is needed to realize facile rotation of phenyl rotors in the solid state, as mentioned in section 5.2.

#### 4.9. Electronic Excited and Charged Species

The structure and the rotational barrier of DPE are considerably affected by the electronic state. The optimized structures of DPE are planar with a linear acetylene axis for the neutral, radical cation, radical anion, and triplet excited ( $T_1$ ) species according to calculations at the HF/4-31G\* level.<sup>65</sup> The triple bond is apparently long in the charged and excited species (1.22–1.26 Å) relative to that in the neutral ground state (1.19 Å). Time-resolved Raman spectra showed that the  $\text{C}\equiv\text{C}$  stretching bands of DPE were shifted to the low wavenumber region in the order of the neutral ground state, radical cation, radical anion, and  $T_1$  species, indicating that the triple bond was dramatically weakened in this sequence.<sup>117</sup> The rotational barrier is dramatically enhanced in the charged and excited species. DFT calculations at the B3PW91/6-311G\*\* level predicted barriers of 50 and 59 kJ/mol for the anion and cation species, respectively (*cf.* neutral species 3.6 kJ/mol).<sup>67</sup> The barrier enhancement is attributed to the breaking of the cylindrical structure of the electron density along the axis of symmetry. Photoelectron spectroscopy revealed that the rotational barrier of DEP was 24 kJ/mol for the ground state cation due to effective  $\pi$  electron conjugation.<sup>118</sup>

#### 4.10. Miscellaneous Effects

The rotational barrier of 2-butyne is slightly enhanced by 5–10% in the excited states of methyl rocking and C–H stretching compared with that in the ground state.<sup>48,49</sup> It is interesting that the rotational barrier of DPE is influenced

by the external electric field.<sup>64</sup> DFT calculations at the B3LYP/6-311+G\*\* level showed that the barrier was enhanced from 3.30 to 4.37 kJ/mol on applying an electric field at  $2.57 \times 10^9 \text{ V m}^{-1}$ . The coplanar conformation is more stabilized than the perpendicular conformation by the induced dipole moment. This function is fascinating in the molecular design of electronic devices.

### 5. Strategic Control of Rotational Isomerism

#### 5.1. Restricted Rotation

The enhancement of rotational barriers in an extended system is a challenging quest in this research area because interactions between the terminal groups are much weaker than those in a nonextended system. Nevertheless, very bulky substituents do enhance the rotational barrier due to destabilization of the transition state of the rotation process by the steric hindrance. For some compounds, the barriers are sufficiently enhanced to allow observation of the dynamic process by NMR spectroscopy. In general, the enhancement is more difficult for acyclic alkynes than cyclic alkynes because of the increased freedom of motion in the former. Some examples of highly restricted rotations are introduced here by structure.

##### 5.1.1. Acyclic Diarylethyne

Because several atropisomers were isolated for 2,2',6,6'-substituted biphenyls,<sup>70</sup> their extended analogues, DPEs with four ortho substituents, are candidates for the realization of the restricted rotation about the acetylene axis. As bromo substituents only slightly enhance the rotational barrier as mentioned in section 4.5,<sup>100</sup> one needs to introduce bulkier groups, such as phenyl groups at the ortho positions. Tetrakis(4-methylphenyl) derivative **19a** takes a nonplanar conformation with a dihedral angle of  $63^\circ$  to avoid steric hindrance between the 4-methylphenyl groups (Figure 14).<sup>119</sup> NMR measurement of its  $C_2$  symmetric analogue **19b** having two 4-methoxymethyl groups showed no line shape changes due to restricted rotation even at  $-100^\circ\text{C}$ , with the upper limit of the barrier being 35 kJ/mol. When two 2,4,6-trimethylphenyl groups were introduced at the ortho positions as wing moieties, the barrier of **20** was enhanced to 51 kJ/mol, as determined by the line shape analysis of the signal due to the 2,6-methyl groups.<sup>120</sup> A higher barrier was observed for DPE derivative **21**, having four (trialkylsilyl)ethynyl groups at the ortho positions.<sup>121</sup> The rotational barrier was estimated to be 78 kJ/mol by analyzing the line shape of the  $^1\text{H}$  NMR signals due to the alkyl groups. These results mean that ethynyl groups possessing large end groups are effective for the restricted rotation relative to the phenyl groups.

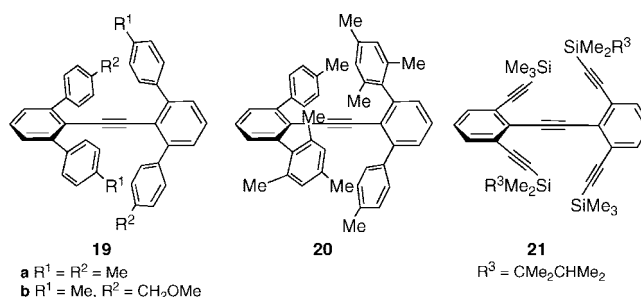


**Figure 14.** DPEs with bulky substituents at all ortho positions.

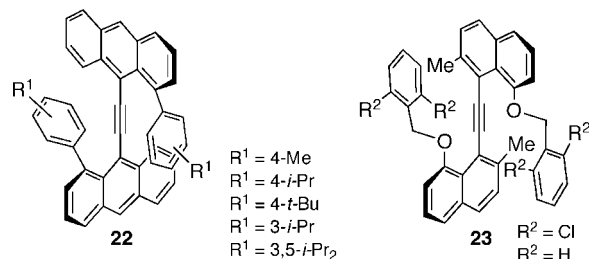


**Figure 15.** Extended bianthryl and naphthyls with bulky substituents.

Polycyclic aromatic moieties can act as rigid rotors in the diarylethyne system. In compounds **22**, which are extended 9,9'-bianthryl derivatives, the two anthryl groups show a staggered arrangement about the acetylene axis to avoid steric interactions with the 1-phenyl groups (Figure 15).<sup>122,123</sup> The rotational barriers about the acetylene axis were determined by the total line shape analysis of the signals due to the substituted phenyl groups. The barriers were in the range of 45–51 kJ/mol, and the highest barrier was found for the 3,5-diisopropyl derivative. Compounds **23**, which are extended 1,1'-binaphthyl derivatives, also prefer to take a staggered conformation because of the steric hindrance.<sup>124</sup> The enantiomerization via the rotation about the acetylene axis results in site exchanges between the diastereotopic methylene protons. This process was nearly frozen at  $-70\text{ }^\circ\text{C}$  to give the barrier height of 49 kJ/mol for the 2,6-dichloro compound. This barrier is higher by ca. 12 kJ/mol than that of the nonsubstituted compound, this meaning that the two chloro substituents are effectively destabilize the transition state. The above rotational barriers are much lower than those of the nonextended analogues,  $>170\text{ kJ/mol}$  for 9,9'-bianthryl<sup>125,126</sup> and 98 kJ/mol for 1,1'-binaphthyl.<sup>127</sup>

### 5.1.2. Acyclic Dialkylethyne

The 9-triptycyl (9,10-benzo-9,10-dihydroanthracene-9-yl) group is known to be extremely bulky, as it possesses three benzo groups fixed in the bicyclic system. This feature has been extensively utilized in the chemistry of stable rotational isomers about the C–C bonds.<sup>128</sup> For example, 9-*tert*-alkyltriptycenes and 9,9'-bitriptycyl are conformationally fixed about the C–C single bonds at the 9-positions even at high temperatures. In particular, the rotational barriers of the latter system are so high that the rotation does not take place at all even at  $300\text{ }^\circ\text{C}$ .<sup>129</sup> Therefore, the extended 9,9'-bitriptycyl, namely, di-9-triptycylethyne (**24**), should be promising to achieve restricted rotation about the long axes.

The  $^1\text{H}$  NMR spectrum of tetramethyl compound **24d** gave two sets of signals due to the *ap* and *sc* forms at room temperature, and the signals became broad at high temperature due to interconversion (Figure 16).<sup>130</sup> The kinetic and thermodynamic parameters of the rotational isomerism of this compound and other derivatives were determined by the dynamic NMR technique (Table 6).<sup>131–133</sup> The rotational barriers range from 42 to 79 kJ/mol depending on the substituents at the 1-positions, and the highest barrier was found for mesityl compound **24j**. For the 1,4-dimethyl derivatives ( $X = \text{Me}$ ), the barrier heights are linearly correlated to the van der Waals radius of the substituents at the 1'-position, as shown in Figure 17. This relationship indicates that the steric size of the phenyl group is ca. 1.8 Å, comparable to that of the methyl group, and is consistent with literature data.<sup>134</sup> The estimated steric sizes are 2.0 and

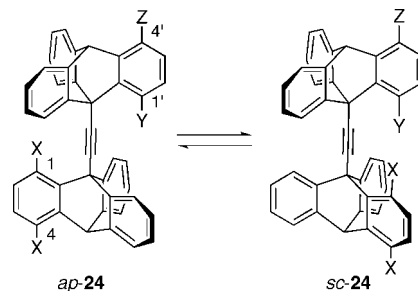


**Figure 16.** Rotational isomerization in di-9-triptycylethyne derivatives. See Table 6 for substituents X, Y, and Z. Stereodescriptors are valid for **24c–24l** and **24n**.

**Table 6.** Kinetic and Thermodynamic Data for Rotation about the Acetylene Axis in Substituted Di-9-triptycylethyne (**24**)<sup>a</sup>

compound	substituent			$\Delta G^\ddagger$ (kJ/mol) <sup>b</sup>	$\Delta G^\circ$ (kJ/mol) <sup>c</sup>
	X	Y	Z		
<b>24a</b>	H	H	H		
<b>24b</b>	Me	H	H	42	
<b>24c</b>	Me	OMe	OMe	53	–1.1
<b>24d</b>	Me	Me	Me	64	3.7
<b>24e</b>	Me	F	H	49	–1.0
<b>24f</b>	Me	Cl	H	62	0.8
<b>24g</b>	Me	Br	H	70	1.8
<b>24h</b>	Me	I	H	72	3.3
<b>24i</b>	Me	Ph	H	66	3.8
<b>24j</b>	Me	Mes	H	79	10.0
<b>24k</b>	Me	–C≡CPh	H	73	2.9
<b>24l</b>	Me	–C≡C(1-naph)	H	74	3.3
<b>24m</b>	OMe	H	H	33 (168K)	
<b>24n</b>	OMe	OMe	OMe	39	–2.0 (168K)

<sup>a</sup> Solvent is  $\text{CDCl}_3$ ,  $\text{CD}_2\text{Cl}_2$ , or 1,1,2,2-tetrachloroethane- $d_2$ . Temperature is 273 K unless otherwise mentioned. See structures in Figure 16 for positions of substituents. <sup>b</sup> Free energy of activation for rotation from *ap* to *sc* isomer or for topomerization. <sup>c</sup> Free energy difference from *ap* to *sc* isomer. Because statistical contribution is considered, the population ratio of *ap* and *sc* isomers is 1:2 when the energy difference is zero.

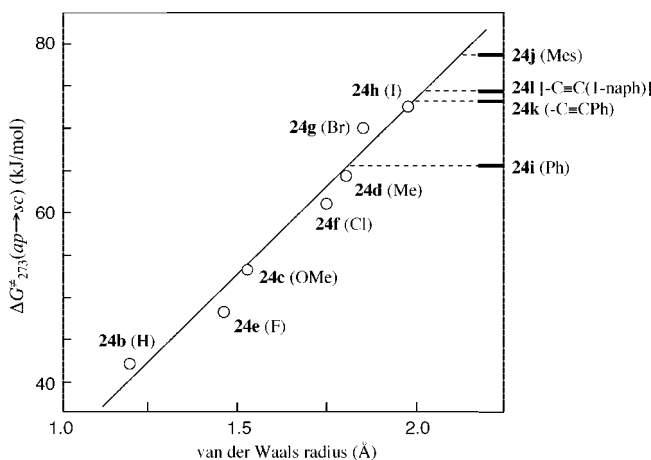


**Figure 17.** Plot of van der Waals radii of 1'-substituent vs free energies of activation of rotation from *ap* to *sc* isomer for **24b–24l**. Adapted with permission from ref 133. Copyright 2001 Elsevier.

2.1 Å for arylethynyl and mesityl groups, respectively. The X-ray analysis and the MM calculations revealed that acetylene carbons in **24** suffered from small bending deformations depending on the combination of substituents: the angles were usually  $>170^\circ$ , except for some derivatives with bulky substituents, such as **24j** ( $166^\circ$  and  $172^\circ$ , X-ray).<sup>133</sup> These deformations should have a minor contribution to the steric energy because of a small bending constant.

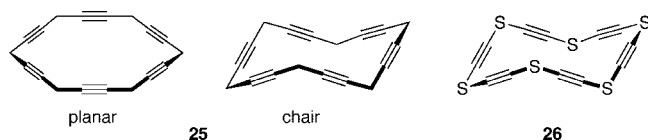


**Figure 18.** Fully extended cyclohexane **25** and its hexathia analogue **26**.

The thermodynamic data in Table 6 indicate that the population of the *sc* isomer tends to decrease with increasing the size of the substituents at the 1-position. However, there are some irregularities in this trend: namely, compounds with OMe and F substituents (**24c**, **24e**, and **24n**) show negative  $\Delta G^\circ$  values (i.e., the population of the *sc* isomer is more than 66%) regardless of the steric congestion. This result is attributed to the intramolecular C–H $\cdots$ O or C–H $\cdots$ F hydrogen bonds that stabilize the *sc* isomer.<sup>135,136</sup> The presence of these interactions is supported by MM calculations: for example, the distance between the interacting H and F atoms is 2.54 Å, which is shorter than the sum of the van der Waals radii of the two atoms (2.67 Å), in the optimized structure of *sc*-**24e**. Systematic analysis of the above kinetic and thermodynamic data gives useful information of the steric effects and the weak molecular interactions.

### 5.1.3. Cyclic Alkylethyne

The conformational interconversion of cyclohexane by concurrent rotation about single bonds was also investigated for the extended system by MM2 calculations. The fully extended cyclohexane **25**, also referred to as [6]pericycline, has comparable energies in the chair, boat, and twist-boat forms, which are more stable by 8 kJ/mol than that in the planar form (Figure 18).<sup>5</sup> This energy relationship is similar to that observed in the corresponding dodecamethyl analogue. These data mean that [6]pericycline is much more conformationally flexible than cyclohexane. In contrast, hexathia derivative **26** has a significant barrier to inversion between chair forms via the half-chair form as the transition state (39 kJ/mol) based on DFT calculations.<sup>137</sup>

### 5.1.4. Cyclic Arylethyne

The restriction of rotation about the acetylenic axis is more easily accomplished in the aromatic cyclic systems than in the other compounds discussed above because of the facile construction of rigid ring systems with decreased freedom of motion. There are several examples of cyclic arylene compounds with acetylene linkers showing restricted motion. The interconversion between stereoisomers results from ring transformation accompanied by the rotation about the acetylene linkers, although it is not always easy to differentiate the two processes. Dynamic processes are classified as shown below according to the shape persistence of the ring structures and the mode of dynamic motion.

**5.1.4.1. Twisting of Helical Molecules.** Some cyclic compounds with arylene groups and acetylene linkers take helical structures that undergo interconversion between the enantiomeric forms via twisting of the framework involving rotation about the acetylene axis.<sup>138</sup> Compound **27**, one of the earliest examples of such structures, consists of two biphenyl units and two acetylene linkers (Figure 19).<sup>139</sup> The chiral  $D_2$  symmetric structure was confirmed by X-ray analysis,<sup>140</sup> while the resolution of the enantiomers has remained unsuccessful. The mobility of such helical systems

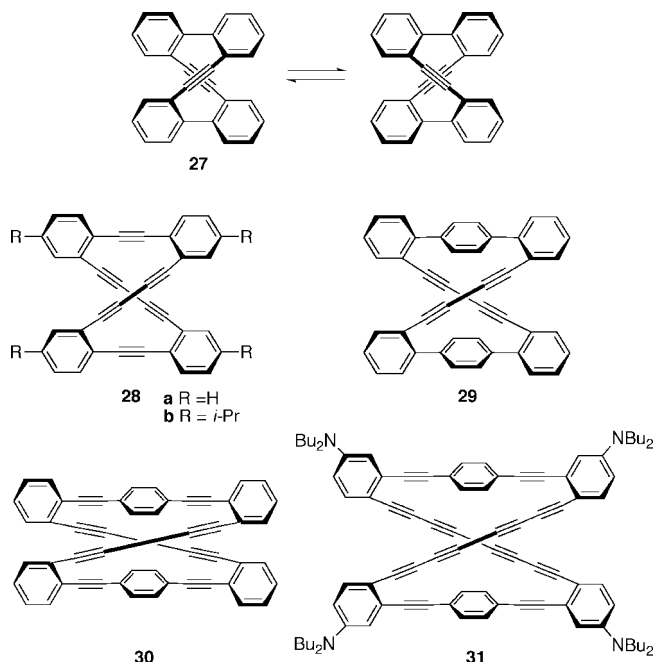


**Figure 19.** Helical cyclic compounds **27–31** and enantiomerization between enantiomeric helical structures of **27**.

is strongly affected by the length and combination of linkers. Compound **28**, with two  $C_2$  and two  $C_4$  linkers, is a unique macrocycle because it exploded violently at 245 °C to give tube- and onion-like carbon particles.<sup>141</sup> The helical structure of **28a** was established by X-ray analysis, while the barrier to enantiomerization between the helical structures was determined by the dynamic NMR method to be 39 kJ/mol for tetraisopropyl derivative **28b**. Compounds **29–31** are examples of helical structures incorporated with *p*-phenylene units (Figure 19). The two phenylene rings are located in a nearly overlapping manner in the X-ray structures of **29** and **30**, where the interlayer distances are 7.0 and 3.6 Å, respectively.<sup>142,143</sup> Molecular modeling suggested that **31** would require a large energy for isomerization between enantiomeric forms via a strained, planar, and rectangular-like intermediate.<sup>144</sup>

Compound **32**, consisting of four *o*-phenylene and two *m*-phenylene units, was obtained as a mixture of isomers in a 3:1 ratio: the major and minor isomers were assigned to bow tie **32a** and butterfly **32b** conformations, respectively, on the basis of the NMR signal pattern (Figure 20).<sup>144</sup> Each isomer is stable, even on heating to 100 °C, indicating a high barrier to interconversion between the diastereomeric forms. The structure of **33b** with six *o*-phenylene units was confirmed by X-ray analysis to be twisted and nearly  $D_2$  symmetric.<sup>145</sup> This molecule is expected to undergo enantiomerization or topomerization via conformational changes, although such possibilities are not mentioned in the literature. Corresponding decamer **33c** takes a less symmetric conformation in the crystal and must be conformationally flexible in solution.<sup>146</sup> In contrast, tetramer **33a** has a saddle-like nonplanar and relatively rigid structure.<sup>145</sup> Compound **34**, an *m*-substituted analogue of **27**, was designed as a potential fragment of a double-helical system (Figure 21).<sup>147</sup> While tetramethoxy compound **34b** existed in the *meso* form in crystals, the interconversion between the *meso* and chiral forms was observed by  $^1\text{H}$  NMR at low temperature (barrier ca. 50 kJ/mol).

Another type of helical structure was constructed by two benzene groups and two or three eneyne linkers (Figure 22).



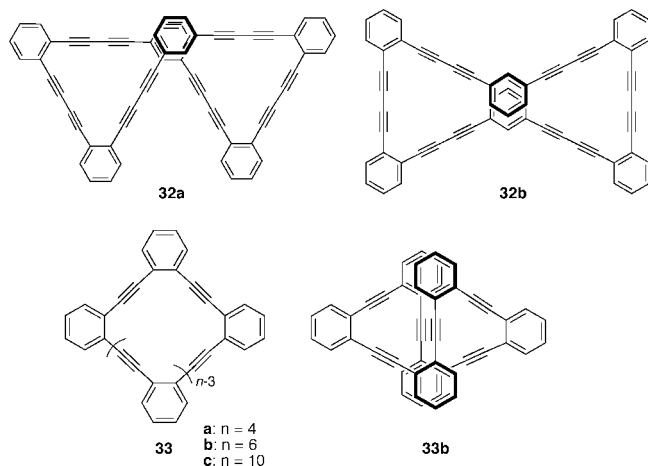


**Figure 20.** Phenylene cyclic oligomers **32** and **33** with acetylene linkers.

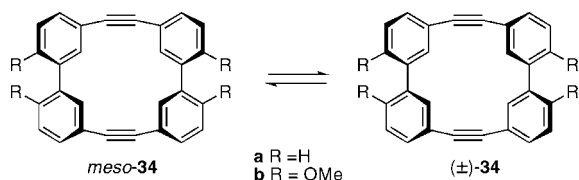


**Figure 21.** Isomerization between *meso* and chiral forms of cyclic compound **34**. Only one of the chiral forms is shown.

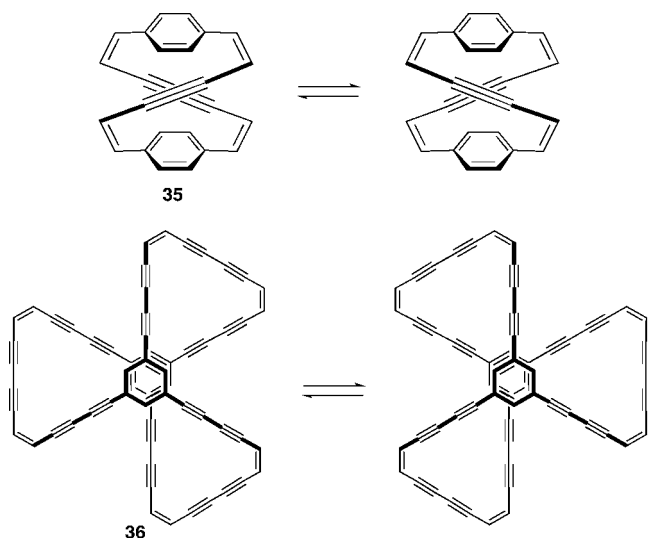


**Figure 22.** Interconversion between enantiomeric twisted forms of cyclic compounds **35** and **36**.

Two benzene rings are connected with two linkers in cyclophane **35**, which prefers to take a twisted conformation.<sup>148</sup> The possibility of resolution of the enantiomers was pointed out, although the barrier to enantiomerization via an untwisted form was not determined. Highly extended helical system **36** ( $C_{60}H_{18}$ ) was constructed with two benzene rings and three  $C_{16}$  enyne linkers.<sup>149</sup> X-ray analysis revealed that the molecule took a nearly  $D_3$  symmetric structure with two benzene rings separated by 3.3 Å. Racemization of the enantiomeric forms proceeds via the rotation of the two benzene planes in the opposite direction. The transition state of  $D_{3h}$  symmetry has 12–26 kJ/mol higher energy than the twisted structures, as predicted by semiempirical and MM methods.

The incorporation of coordination sites into a macrocyclic structure considerably influences the conformational mobility

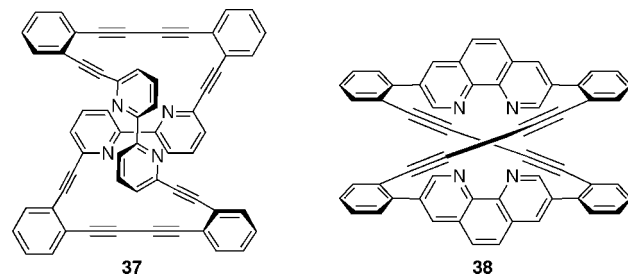


**Figure 23.** Cyclic oligomers **37** and **38** with coordination sites.

by the addition of metal ions (Figure 23). Compound **37** with two 2,2'-bipyridyl units exists as a mixture of several twisted conformers, and the freedom of motion of the macrocyclic ring is decreased by coordination to such metal ions as  $Cu^{2+}$  and  $Ag^+$ .<sup>150</sup> Phenanthroline cyclophane **38** undergoes enantiomerization between twisted conformations via ring inversion at a barrier of <39 kJ/mol.<sup>151</sup> Upon the addition of  $Cu^+$ , the barrier was enhanced to 57 kJ/mol due to stabilization of the helical structure by complexation, as revealed by variable temperature (VT)  $^{13}C$  NMR analysis. However, this barrier is not sufficiently high to allow isolation of enantiopure forms.

**5.1.4.2. Swing and Pedaling.** Anthrylene units are utilized to construct fascinating cyclic structures by taking advantage of the rectangular shape and the possibilities of connection sites. Cyclic 1,8-anthrylene tetramer with four ethynylene linkers **39** adopted a diamond prism structure in the crystals, as revealed by X-ray analysis, where the interlayer distance between the facing anthracenes was ca. 3.4 Å (Figure 24).<sup>152,153</sup> This compound showed a dynamic process between two possible diamond structures via the concurrent rotation of the four linker moieties. The barrier to skeletal swing was estimated by VT  $^1H$  NMR measurements to be 38 kJ/mol. The relatively high barrier is attributed to the  $\pi \cdots \pi$  interactions between the facing anthracene moieties in the diamond form. This dynamic behavior is influenced by the

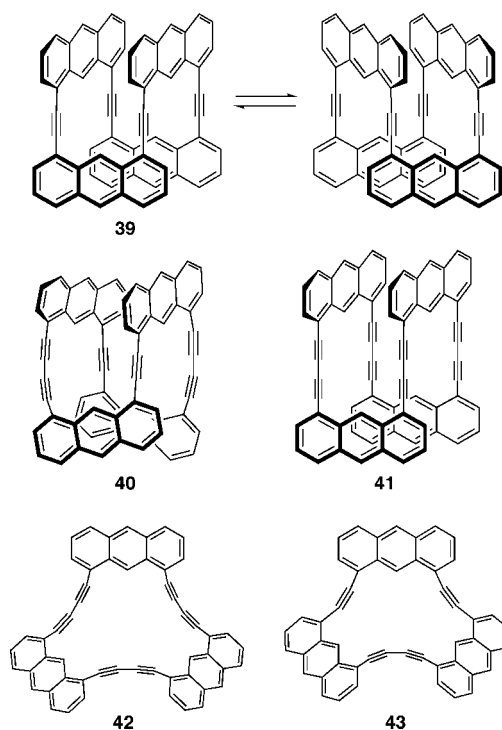


**Figure 24.** Various anthrylene-ethynylene cyclic oligomers **39**–**43** and swinging motion of **39**.

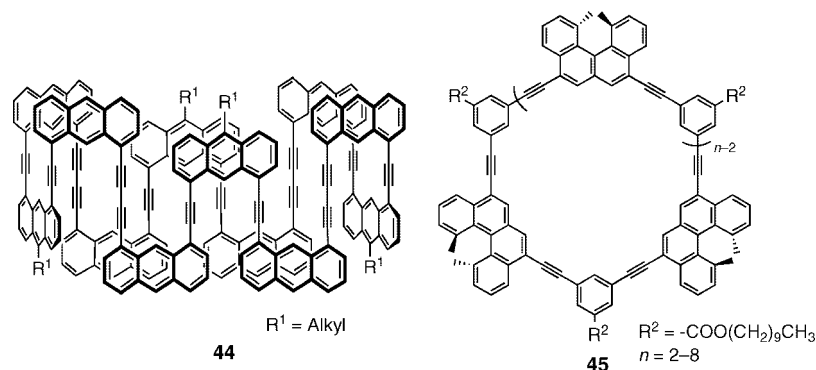


**Figure 25.** Macrocyclic arylene-ethynylene oligomers **44** and **45**.

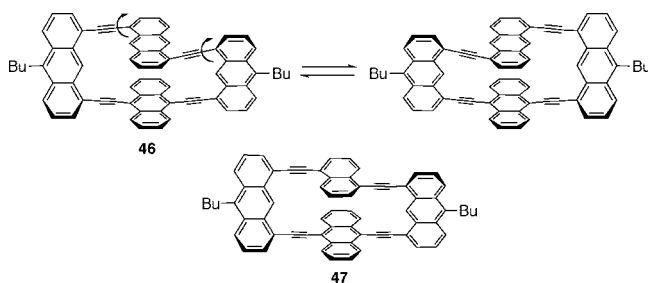


**Figure 26.** Chiral anthrylene-ethynylene cyclic tetramer **46** and its naphthylene analogue **47**.

incorporation of diacetylene linkers into the cyclic structure.<sup>154</sup> Tetramer **40** with two longer linkers exists as one diamond form solely, and enantiomers of this chiral oligomer were successfully resolved by chiral HPLC. In contrast, all-diacetylene tetramer **41** undergoes the skeletal swing rapidly even at low temperature. Cyclic trimers **42** and **43** adopt nonplanar and strained ring structures.<sup>155</sup> The former exists in the  $C_2$  symmetric form, which undergoes very rapid pseudorotation-like motion in solution. The degree of freedom of the cyclic system increases with increasing number of arylene units. Actually, 1,8-anthrylene dodecamer **44** with acetylene and diacetylene linkers exhibited temperature dependence in its  $^1\text{H}$  NMR spectra, indicating the presence of a large number of conformers in solution (Figure 25).<sup>156</sup> A similar conformational change was also observed in higher helicene oligomers **45**: octamer ( $n = 8$ ) had a flexible structure while smaller analogues ( $n = 2-7$ ) had rigid structures.<sup>157</sup>

Cyclic tetramer **46** features a chiral structure containing 1,5- and 9,10-anthrylene units, and undergoes racemization via rotation of the 1,5-anthrylene units about the acetylene linkers (Figure 26).<sup>158,159</sup> The barrier to this pedaling motion is so high that the enantiomers could be resolved by chiral HPLC at room temperature. The barrier to racemization was determined by classical kinetics to be 114 kJ/mol. In contrast, 1,5-naphthylene analogue **47** undergoes a similar dynamic process very rapidly at low temperature because of the decreased bulkiness of the crank moiety.

**5.1.4.3. Shape-Persistent Framework with Rotors.** Beard and Moore proposed the molecular design of a “molecular turnstile”, which consisted of a rigid macrocyclic phenylene-ethynylene framework and a spindle *p*-phenylene moiety as shown in Figure 27.<sup>160</sup> Compounds **48** prefer to take a nonplanar conformation because of the steric interactions between substituents attached to the spindle and the macrocycle. The rates of rotation were monitored by measuring  $^1\text{H}$  NMR signals due to the diastereotopic methylene protons. The barriers to rotation were estimated to be 56 kJ/

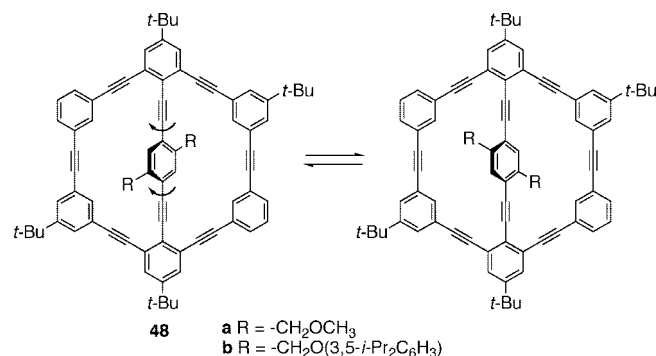


**Figure 27.** Isomerization of molecular turnstiles **48** via rotation of the spindle moiety.

mol for **48a** and >86 kJ/mol for **48b**, and a locked spindle was achieved in the latter.

Macrocyclic compound **49** with four *m*-phenylene and two *p*-phenylene moieties has a shape-persistent scaffold where interconversion between diastereomers via rotation of the *p*-phenylene groups takes place much faster than the NMR time scale at room temperature (Figure 28).<sup>161</sup> Compounds **50** and **51** have 9,10-anthrylene units that can rotate along the macrocyclic rings.<sup>162</sup> Whereas the X-ray analysis of **50** showed a nonplanar structure with rotation of the anthrylene units from the averaged plane of the framework, the calculations suggested that the rotation required a small energy, ca. 8 kJ/mol per unit. Compound **51** features strong self-association in chloroform solution because of  $\pi\cdots\pi$  stacking interactions. Compound **52** bears three triptycene-9,10-diyl rotors within a rigid trigonal prism framework constructed by pyridyl ligands and six Pt atoms.<sup>163,164</sup> MM calculation revealed that this self-assembled system furnished inner space sufficiently for the rotation of the triptycene paddle wheels. Actually, the rotation occurred rapidly on the NMR time scale.

Cyclic *p*-phenylene-ethynylene oligomers are a novel class of strained  $\pi$ -conjugated compounds, and compound **53** is an example of a hexamer (Figure 29). Some derivatives feature the inclusion of guest molecules, such as fullerenes, into their central cavities.<sup>165,166</sup> Hexamer **54**, with six 1,4-naphthylene units, exists as a mixture of eight possible conformers with rapid interconversion, but its conformational mobility is restricted in the  $C_{60}$  complex. The flipping of one naphthalene ring along the bent acetylene axis while maintaining the complexation was observed at low temperature by VT  $^{13}\text{C}$  NMR measurements of a complex with  $^{13}\text{C}$ -enriched  $C_{60}$  ( $\Delta G^\ddagger$  49 kJ/mol).

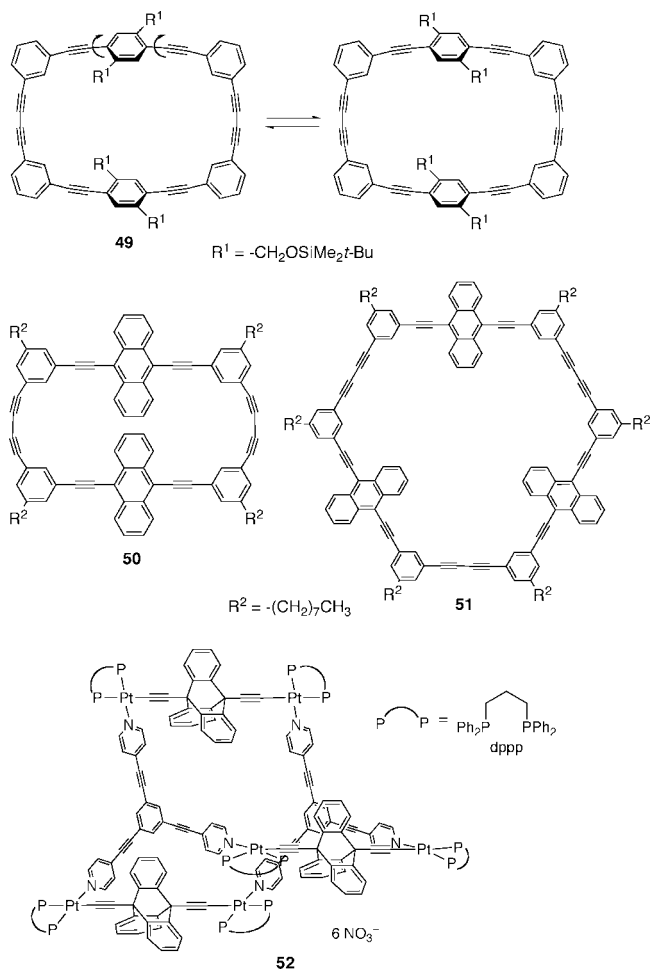


**Figure 28.** Cyclic compounds bearing rotors along macrocyclic frameworks.

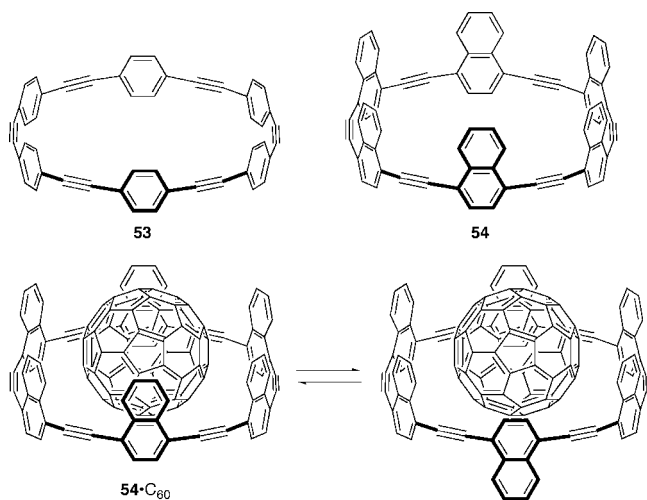


**Figure 29.** Cyclic phenylene and naphthylene oligomers **53** and **54** and dynamic process observed in a complex of **54** with C<sub>60</sub>.

### 5.1.5. Metalated Alkynes

Complexes **55** and **56** (Figure 30) have different metal atoms at both ends of the alkyne moiety.<sup>167</sup> In the <sup>31</sup>P NMR spectra, these complexes showed two signals due to two phosphine ligands attaching to the Pd or Rh atom at low temperature, which broadened and became a sharp single peak upon averaging the temperatures. These phenomena were attributed to restricted rotation about the acetylene axis. The rotational barriers were determined from the coalescence

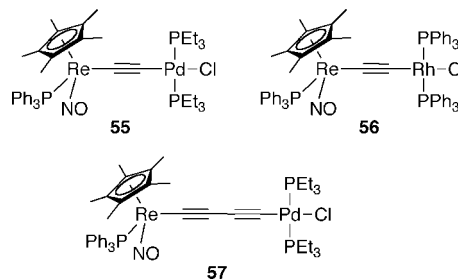


**Figure 30.** Dimetallic alkyne complexes **55**–**57**.

temperature to be 49 and 46 kJ/mol for **55** and **56**, respectively. Diyne derivative **57** did not show similar dynamic behavior, indicating facile rotation about the diacetylene axis.

## 5.2. Facilitated Rotation in the Solid State

As mentioned in section 4.8, the rotation about the acetylene axis is considerably retarded in the solid state because of tight intermolecular contacts in the crystal lattice or packing. Therefore, a strategic molecular design is required to facilitate the rotation in the solid state. Garcia-Garibay and co-workers proposed such a design for molecular gyroscopes or compasses, which consists of an arylene rotor and bulky stator moieties (Figure 31).<sup>168,169</sup> The fundamental assembly is 1,4-bis[(triphenylmethyl)ethynyl]benzene (**58**), where the *p*-phenylene unit can rotate about two ethynylene linkers.<sup>170,171</sup> Theoretical calculations suggested that the rotational barrier of the rotor was negligibly low for an isolated molecule. The dynamic processes in the solid state were observable by VT measurements of <sup>13</sup>C CPMAS NMR or <sup>2</sup>H NMR quadrupolar-echo line shape analysis with a deuterated sample. The activation energies of benzene clathrates of **58a** and **58b** are 54 and 49 kJ/mol, respectively,<sup>170–172</sup> and the rotation takes place rapidly in dodeca-*t*-Bu compound

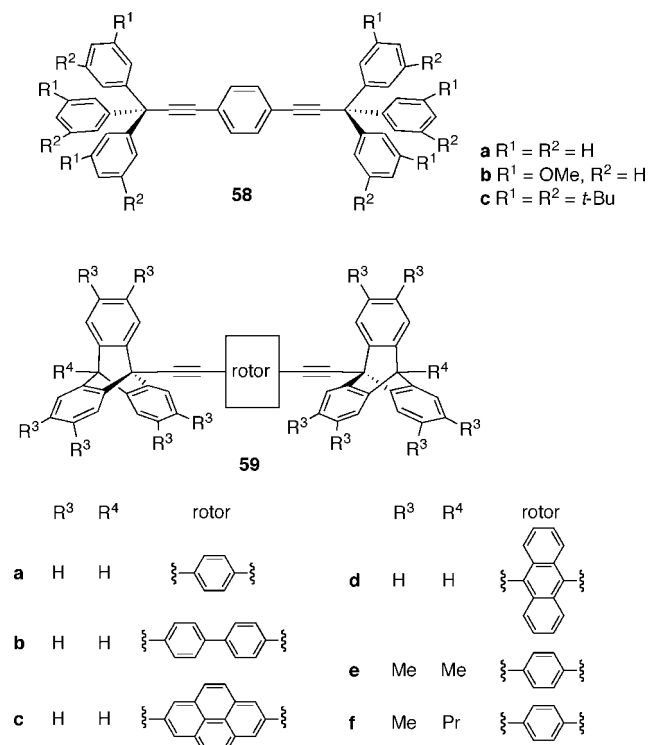


**Figure 31.** Core structures of molecular gyroscopes with *p*-phenylene and a related rotor.



**58c** on the NMR time scale ( $k > 10 \times 10^8 \text{ s}^{-1}$ ).<sup>173</sup> This trend clearly suggests that the bulky stators prevent neighboring molecules from interacting with the rotor moiety in the crystal lattice. The rotational barriers of desolvated forms of **58a** are 47–61 kJ/mol, indicating a relatively small effect of the presence of solvated molecules.<sup>171</sup> These values are reasonably reproduced by MM calculations using a partially relaxed model (ca. 67 kJ/mol), while they are very much overestimated in a rigid lattice approximation (ca. 310 kJ/mol).<sup>174</sup> Therefore, the correlated motion plays an important role in the low barrier rotation in the crystals. A dirotor system consisting of two 1,4-bis(triptylethynyl)benzene structures in a molecule was designed, and the phenylene rotation in a deuterated analogue was found to take place at a rate of  $>10^8 \text{ s}^{-1}$  at 240 K by the  $^2\text{H}$  NMR technique.<sup>175</sup> A triply bridged derivative of the bis-trityl compound was successfully synthesized to obtain a real gyroscope structure.<sup>176</sup>

Triptycyl groups are also used as stator fragments by taking advantage of the rigid bicyclic framework (Figure 31). AM1 calculations of 1,4-bis(9-triptycylethynyl)benzene (**59a**) suggested frictionless rotation of the phenylene moiety about the acetylene axis (barrier  $<0.2 \text{ kJ/mol}$ ), meaning that it is a free rotor even at 25 K.<sup>177</sup> This situation was also found in analogous compounds **59b** and **59c** with biphenyl and pyrene rotors, respectively, while anthracene derivative **59d** had a small barrier of 16 kJ/mol. In the solid state, the phenylene rotor in **59a** is static, as revealed by the  $^{13}\text{C}$  NMR spectra, because of the high packing coefficient, that prevented motions correlated with neighboring molecules.<sup>169</sup> To increase the free space around the rotor moiety, highly alkylated derivatives **59e** and **59f** were also synthesized from the corresponding alkylated 9-ethynyltriptycene.<sup>178</sup> The  $^2\text{H}$  NMR spectra of compound **59f** with a deuterated phenylene rotor were measured at 150–183 K to give an activation barrier of 18 kJ/mol.<sup>179</sup> A hybrid-type gyroscope with an asymmetric triptycyl–trityl stator showed faster rotational dynamics (33 kJ/mol) than the ditriptyl compound.<sup>180</sup>

### 5.3. Folding of Acyclic Alkynes

#### 5.3.1. Helicates

Chains of *m*- or *o*-phenylene–ethynylene (*m*PE and *o*PE) oligomers are conformationally flexible under ordinary conditions because of the facile rotation about the acetylene axis. As illustrated in Figure 32, each side of the oligomeric zigzag is ca. 4.5 times as long as that of an alkane chain. Such oligomers should exist as a mixture of a large number of conformers. However, the molecules can fold into well-

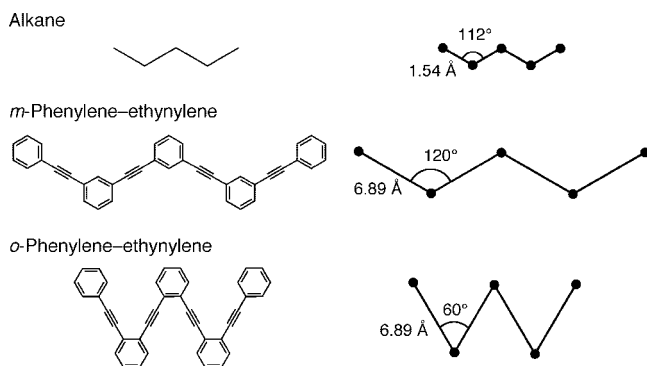


**Figure 32.** Schematic presentations of zigzag conformations of *m*- and *o*-phenylene–ethynylene oligomers and a straight-chain alkane.

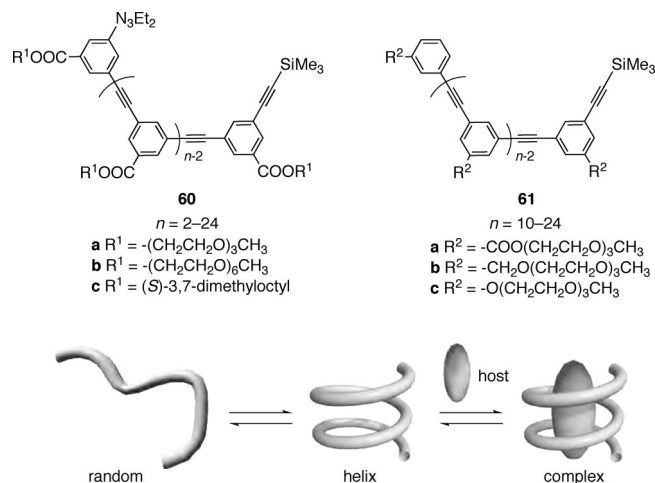


**Figure 33.** *m*-Phenylene–ethynylene oligomers with various long side chains **60** and **61** and schematic diagrams of a folding oligomeric chain accompanying complexation of a guest molecule.

defined conformations, such as a helix, upon introduction of appropriate side chains based on solvent effects and other molecular interactions. Molecular models suggest that one helical cycle needs ca. 7 and 4 repeating units (including terminal units) for the *m*PE and *o*PE oligomers, respectively, being reflected by the angles at the corners.

Compounds **60a** and **60b** consist of a *m*PE chain and ethylene glycol side chains at the benzoic acid units (Figure 33). These molecules form a helical coil in chloroform, as detected by UV and NMR spectroscopy, while such a phenomenon was negligible in acetonitrile.<sup>181,182</sup> Observations due to intramolecular  $\pi \cdots \pi$  stacking become significant when the chain length is greater than 8, being consistent with the geometrical requirement. The degree and mode of the folding of *m*PE oligomers are influenced by the nature of side chains and phenylene moieties. The oligomer with ester side chains (**61a**;  $n = 18$ ) prefers to adopt a helically folded conformation in a range of solvents, whereas those with benzylic and phenolic ether side chains (**61b** and **61c**;  $n = 18$ ) have only limited ability for  $\pi$ -stacking.<sup>183</sup> Oligomers with the ester side chain and terminal pyridyl units undergo cooperative self-assembly by coordination to Pd atoms.<sup>184</sup> The twist sense of these chiral helices can be biased into one helical form by various ways. When oligomers with enantiopure tethers or side chains, for example **60c**, were dissolved in appropriate solvents, the solutions gave induced bands in the CD spectra, which are evidence of enantiomeric bias.<sup>185–187</sup> Achiral oligomeric chains can form CD active complexes with enantiopure guests. A dodecamer with long hydrophilic chains (**60b**;  $n = 12$ ) accommodates  $\alpha$ -pinene in its hydrophobic interior cavity with the helical conformation in aqueous acetonitrile, as illustrated in Figure 33.<sup>188,189</sup> Long achiral oligomers **61** ( $n = \text{ca. } 20$ ) form well-ordered helical structures around a rodlike diamine molecule.<sup>190</sup>

An intramolecular hydrogen bond is utilized in the construction of rigid backbones in *m*PE oligomers with bonding sites, as mentioned in section 4.6.<sup>103,104</sup> Oligomers up to the heptamer (for example, hexamer **62** in Figure 34) were found to be helical even in nonpolar solvents such as chloroform. This feature was confirmed by NMR and UV spectroscopy: for example, NOE contacts between end groups in the oligomeric chain were observed for pentamer and higher oligomers, being consistent with the helical geometry.

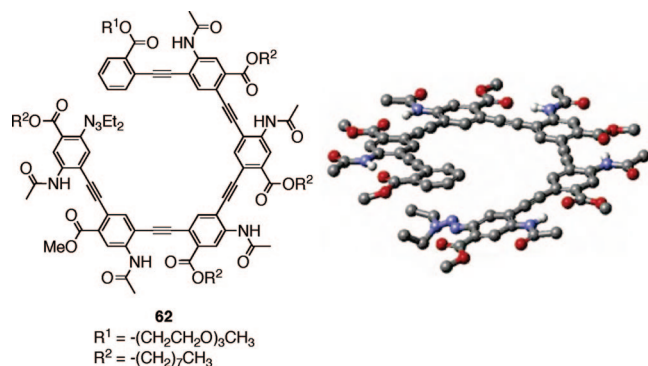


**Figure 34.** Conformationally rigidified *m*-phenylene-ethynylene hexamer by intramolecular hydrogen bonds and calculated structure of an all-methyl-ester compound by MM3. Adapted with permission from ref 104. Copyright 2004 American Chemical Society.

Oligomers based on an *o*PE chain can form helical structures where each linear unit is connected to the next one at small angles (ca. 60°). For example, tetramer **63** with polar side chains adopts a helical conformation in acetonitrile, as confirmed by NMR spectroscopy (Figure 35).<sup>191</sup> Longer oligomers **64**, hexamer and nonamer, with polar and nonpolar substituents also undergo folding into helical conformations in solution.<sup>192</sup> NMR and CD measurements revealed that oligomers **65** up to nonamer adopted a helical conformation in heptane, while they adopted extended conformations in chloroform.<sup>193</sup> This phenomenon is attributed to solvophilic effects of the nonpolar enantiopure alkoxy groups in the oligomeric chain. Compound **66** has longer linkers (ca. 11 Å) between *o*-phenylene units bearing dodecyloxy side chains.<sup>194</sup> The spectral features in cyclohexane are consistent

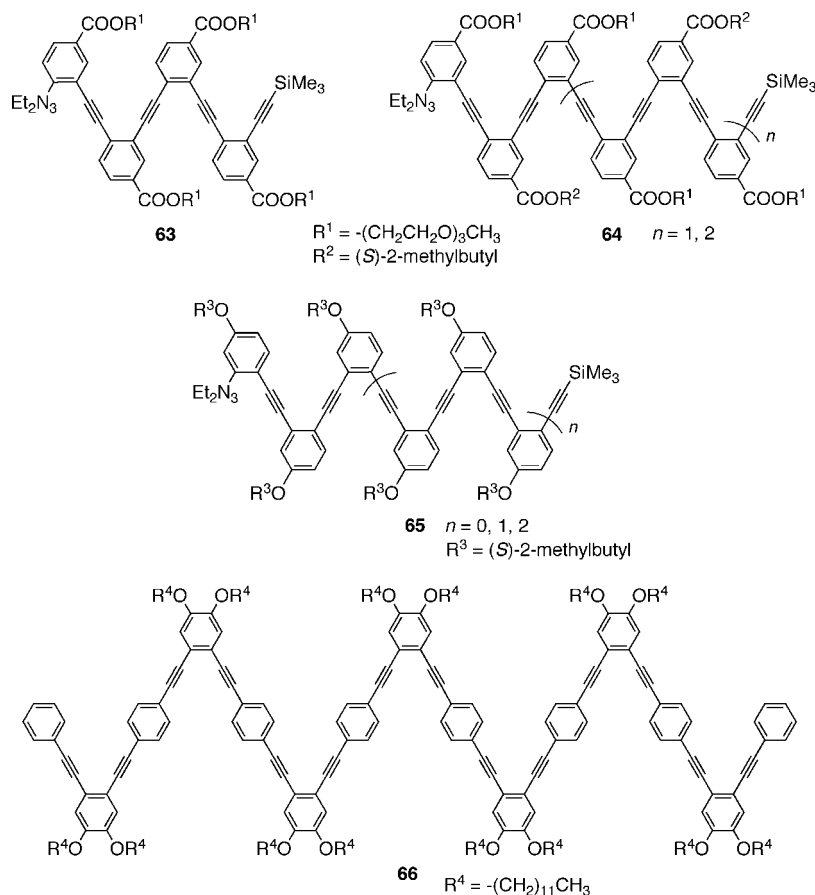


**Figure 35.** *o*-Phenylene-ethynylene oligomers **63**–**66**.

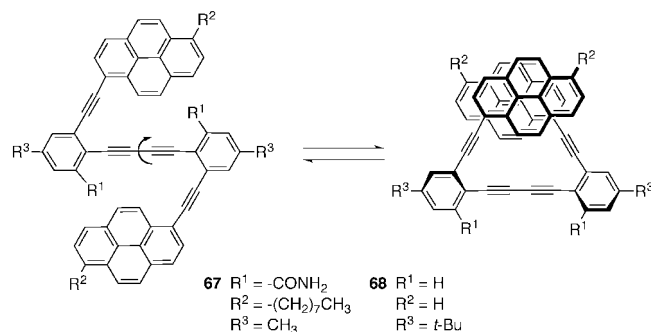


**Figure 36.** Interconversion between open and closed forms of molecular hinges **67** and **68**. Only one enantiomeric form is shown for the closed conformation.

with a folded compact conformation, possibly a triangle-like helical structure with a large interior.

### 5.3.2. Molecular Hinges

Acetylene linkers are utilized as a pivot connecting two plate moieties in molecular hinges. The mobility and the preferred conformation are controlled by the nature of the wing substituents. Although compound **67** undergoes rapid rotation about the diacetylene linker, the conformation is fixed in the presence of diamine due to the complexation via a hydrogen bond, where the two pyrene moieties come close to each other (Figure 36).<sup>195</sup> Induced CD bands were observed in the region of the pyrene band upon the addition of an enantiopure diamine, meaning that the two enantiomeric forms of the closed formation exist in an unequal ratio under the given conditions. Compound **68** formed two types of crystals upon recrystallization from hexane, and X-ray

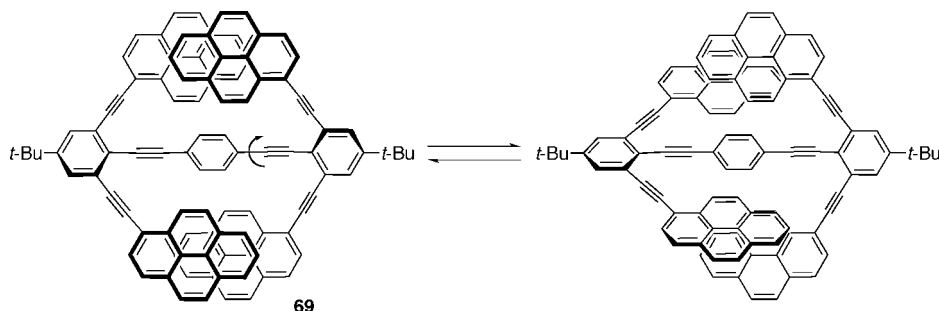


**Figure 37.** Dynamic process between  $\pi$  stacking and nonstacking forms of **69**.

analysis revealed that the crystals had different conformations, open and closed forms.<sup>196</sup> In solution, the two forms are in equilibrium and the closed form is predominant at room temperature due to  $\pi\cdots\pi$  interactions between the pyrene moieties. Compound **69** with four pyrene moieties and a longer linker prefers to take a closed form with two pairs of  $\pi$ -stacking interactions between pyrenyl groups (Figure 37).<sup>197</sup> The dependence of the equilibrium between the two forms on the temperature could be monitored from the chemical shifts of the <sup>1</sup>H NMR signals.

## 5.4. Tuning of Photophysical Properties

Acetylene linkers play an important role in extending the conjugation between terminal  $\pi$  systems. Therefore, the conformation about the acetylene axis, namely dihedral angles between the terminal groups, influences the photophysical properties of diarylethynes and their longer analogues. The effects of conformation on DPE have already been mentioned in section 4.4. This section treats two other examples involving larger  $\pi$  systems.

### 5.4.1. Bis(phenylethynyl)anthracene Chromophores

9,10-Bis(phenylethynyl)anthracene (**70**) and its derivatives are highly fluorescent ( $\Phi_f$  0.85 for **70** in benzene)<sup>198–200</sup> and useful fluorophores or light emitters in sensor and device chemistry (Figure 38). Their emissive properties are tunable by the structure and conformation of the terminal groups as well as the conditions. According to AM1 calculations, the global minimum structure of **70** is fully coplanar, and the perpendicular conformation is less stable by only 1.4 kJ/mol than the global minimum.<sup>201</sup> The conformational change from the coplanar form to the perpendicular one results in a blue-shift of 32 nm for the absorption band at the longest wavelength, as predicted by ZINDO/S calculations. The UV–vis spectrum of this compound shows poorly resolved

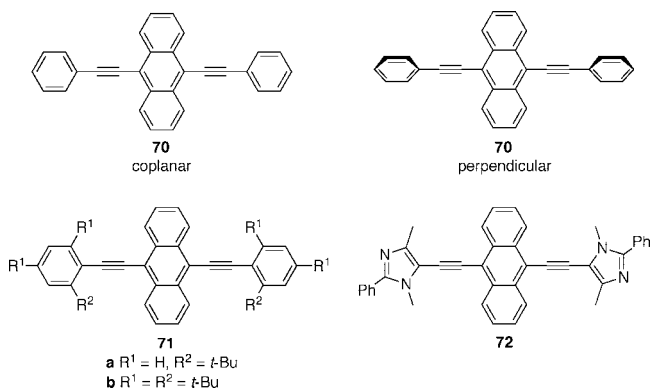


**Figure 38.** 9,10-Bis(phenylethynyl)anthracene **70** and its analogues **71** and **72**.

bands in solution due to the presence of several conformations. In contrast, molecules exist in the planar conformation in a polymer film, showing well-resolved bands. Compounds **71** give information on the effects of the *tert*-butyl groups at the *o*-positions on the structures and electronic spectra.<sup>202</sup> In the X-ray structure of compound **71a**, the two phenyl groups are orthogonal to the anthracene and the two *tert*-butyl groups are *anti* relative to the anthracene plane. Compounds **70** and **71a** showed very similar UV–vis spectra, a broad absorption band, as well as fluorescence spectra at room temperature. A significant hypsochromic shift as well as appearance of distinct vibrational bands was observed in the absorption spectra of **71b** that carried *tert*-butyl groups at all the ortho positions. Such conformational changes were also applied to the photophysical properties of 9,10-diethynylanthracenes with terminal imidazolyl groups.<sup>203</sup> DFT calculations suggested that the dihedral angles between the anthracene and the imidazolyl groups were 14° in the global minimum structures of **72**. Its UV–vis and fluorescence spectra are considerably influenced by the addition of trifluoroacetic acid because of the preference for the twisted conformation by the protonated dication species.

### 5.4.2. Porphyrin Chromophores

Porphyrin chromophores give characteristic absorptions in the visible light region, the B band (or Soret band) and the Q-band. The interactions between multiple chromophores via acetylene linkers lead to significant effects on the absorption bands depending on the modes of connectivity.<sup>204,205</sup> For example, when two porphyrin moieties are connected with a diacetylene linker at the meso positions as in **73** (Figure 39), the B band is split and the Q-band is red-shifted and intensified relative to those in a monomeric model compound due to coupling between the two chromophores. The absorption bands of such dimers also depend on the concentration, the solvent, and the presence of amines because these conditions influence the conformation and aggregation states of extended  $\pi$ -conjugated systems. Theoretical calculations suggested that butadiene dimer **74** preferred to adopt the coplanar conformation with a low rotational barrier (Figure 39).<sup>206,207</sup> The calculated rotational barrier was 4 kJ/mol (AM1) for butadiene dimer **75**.<sup>208</sup> Recent DFT calculations indicated that butadiene dimer **76** had a very low barrier, 2.9 kJ/mol (B3LYP/6-31G\*), in the ground state, while the barrier was enhanced to 16.4 kJ/mol in the first excited state.<sup>209</sup> Actually, the absorption spectrum of this dimer is an average of a broad distribution of conformations. In a similar butadiene dimer, spectroscopic measurements suggested that each conformer could be excited selectively due to inhibition of torsional rotation about the linker in a viscous



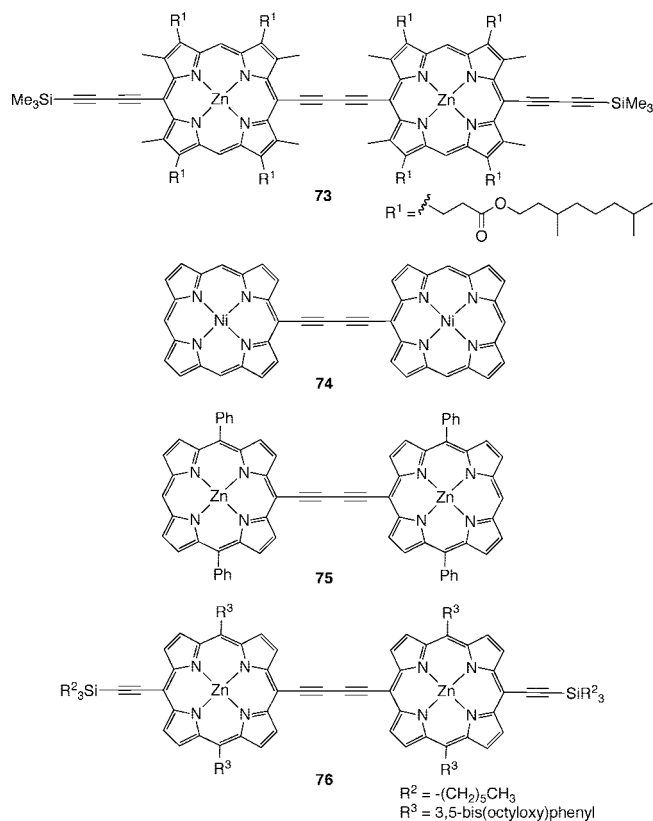


**Figure 39.** Porphyrin dimers connected by diacetylene linkers at meso positions.

medium.<sup>210</sup> This phenomenon plays a significant role in producing singlet oxygen by photosensitization.

The rotational barrier in ethynylene bridged porphyrin dimer **77** is ca. 2 kJ/mol (AM1), while the coplanar conformation is an energy maximum, in contrast to the case of the diacetylene derivative (Figure 40).<sup>208</sup> The electronic coupling between the terminal chromophores in **77** is larger than that in the butadiene analogue. The conformational analyses of porphyrin dimers connected at various positions, *meso* and  $\beta$  positions, were similarly carried out for the analogues of **75** and **77**.<sup>208</sup> In dimers **78**, the two porphyrin moieties are connected with longer linkers involving *p*-phenylene groups. Their rotational barriers were obtained by analysis of direct dipole interactions in the <sup>1</sup>H NMR spectra.<sup>211</sup> The observed values are 2.4 kJ/mol and ca. 0.5 kJ/mol for **78a** and **78b**, respectively, in agreement with those for DPE and 1,4-diphenylbutadiyne (see sections 3.2 and 4.3). Dimers with one metalated porphyrin and one free-base porphyrin are attractive compounds in designing molecular photonic devices, because of facile triplet energy transfer.<sup>212,213</sup> The rate and efficiency of energy transfer are influenced by the nature of linker moieties. DFT calculations of dimers **79** and their bimetalated derivatives showed that the electronic coupling between the two porphyrins was sensitive to the conformation of the central arylene rotor about the acetylene linkers.<sup>214</sup>

## 6. Applications of Rotation about Acetylene Axis

### 6.1. Molecular Vehicles

An ethynyl group with a spherical group, such as fullerene or a 9-triptycyl group, is used as the axle-wheel part in molecular vehicles by taking advantage of the facile rotation

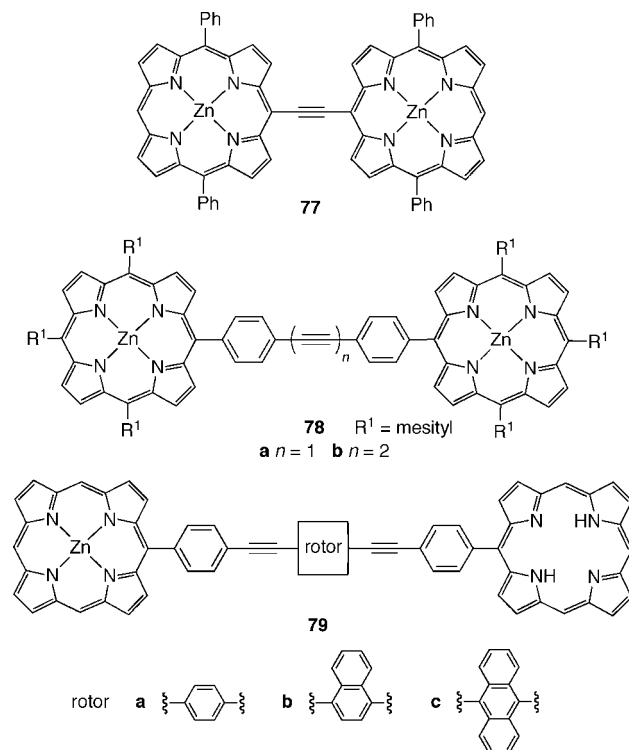


**Figure 40.** Porphyrin dimers with acetylene and diacetylene linkers.

of the wheels relative to the chassis moiety (Figure 41). The rapid rotation was supported by MO calculations of a model compound: the rotational barrier in (phenylethynyl)dihydrofullerene- $C_{60}$  (**80a**) was 1 kJ/mol at the HF/3-21G level (Figure 40).<sup>215</sup> The barrier was slightly enhanced to 4 kJ/mol in 2,5-dimethoxyphenyl derivative **80b** because of the weak intramolecular C–H...O interactions in the energy minimum conformation. As for 9-triptycyl wheels, 1,4-bis(9-triptycylethynyl)benzene (**81a**) (wheel length 11.0 Å)<sup>216</sup> and its terphenyl analogue **81b** (19.7 Å)<sup>217</sup> are adopted in molecular wheelbarrows. It is striking that the rolling motion of di-9-triptycylbutadiyne (**82**) (6.8 Å) was observed by scanning tunneling microscopy (STM) on a Cu surface at the molecular scale in real time.<sup>218</sup> Other modes of motion,

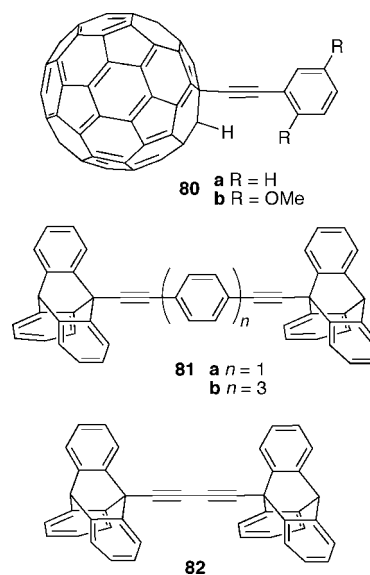


**Figure 41.** Model compounds for axle-wheel parts in molecular vehicles.

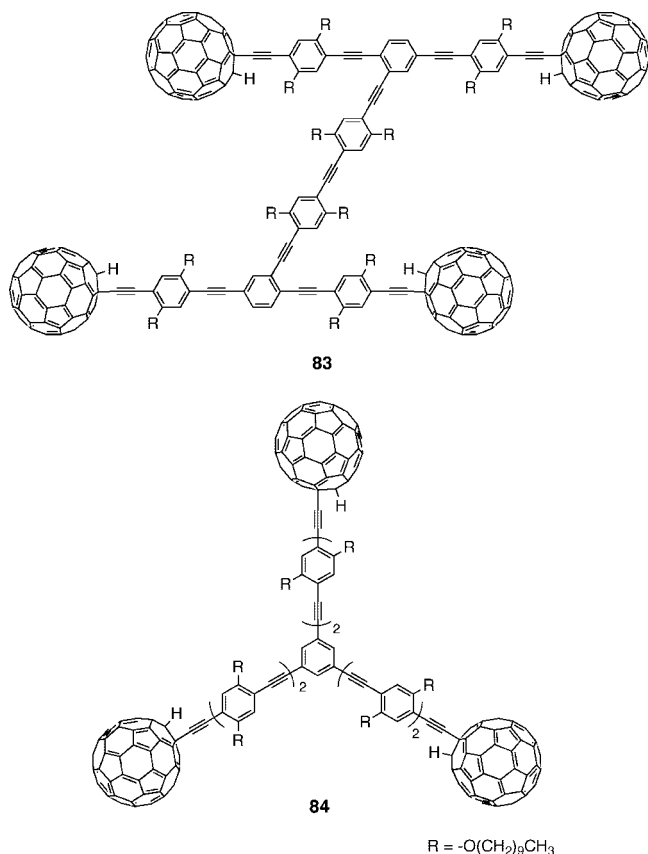


**Figure 42.** Nanocars **83** and **84** with  $\text{C}_{60}$  wheels.

pushing and pulling, were also observed depending on the relative orientation of the molecule relative to the surface and the STM tip.

Tour and co-workers have developed various types of nanocars consisting of chassis, axles, and wheels.<sup>219,220</sup> Compound **83** possesses a phenylene-ethynylene chassis and four  $\text{C}_{60}$  wheels (Figure 42).<sup>215,221</sup> This molecule showed thermally induced translational motion on a gold surface as monitored by STM. The mode of motion can be modified by the direction and number of  $\text{C}_{60}$  wheels and the shape of the chassis. For example, a nanocar bearing three wheels **84** and its four-wheeled analogue with a porphyrin chassis undergo pivoting motion on the surface.<sup>221,222</sup> When an angled chassis is incorporated into ordinary four-wheeled nanocars, the molecules should undergo circular motion rather than translation.<sup>223</sup> A new type of nanocar with *p*-carborane wheels has been designed to improve the solubility and the yields of the reactions to introduce the wheels. Various nanocars with four *p*-carborane wheels (e.g., **85** in Figure 43) and its three- and six-wheeled models were synthesized in reasonable yields with no or short alkyl chains to increase solubility.<sup>224,225</sup> One fascinating example of *p*-carborane analogues is driven by a light-powered unidirectional molecular motor, as the small wheels do not absorb light required for the motor, contrary to fullerene wheels.<sup>226</sup> A new type of nanocar **86**, having different front (*p*-carborane) and back ( $\text{C}_{60}$ ) wheels, was recently reported.<sup>227</sup> The use of other wheels, e.g., a Ru complex, was also proposed.<sup>228</sup>

## 6.2. Molecular Wires

Molecular wires consisting of DPE units are attracting considerable attention in the chemistry of organic electronics.<sup>229</sup> As a model compound, the torsional motion of 1,4-

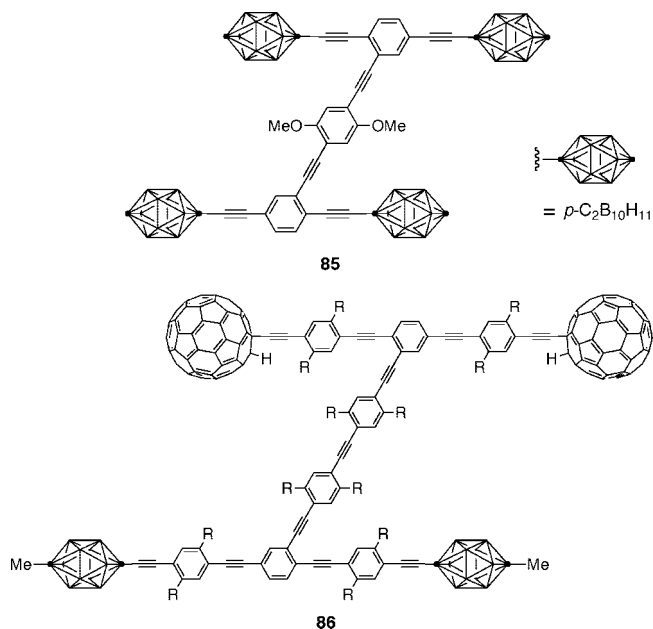


**Figure 43.** Nanocars **85** and **86** with *p*-carborane wheels.

bis(phenylethynyl)benzene (**87**) was extensively investigated by various methods (Figure 44). AM1 calculations indicated that the fully planar structure was more stable by only 2 kJ/mol than the twisted structure and the energy difference in the excited state was much larger than that in the ground state.<sup>230</sup> Bathochromic effects were observed in the absorption and emission bands in the following order: the twisted form, the coplanar form, and the aggregated coplanar form. The rotational barrier of this compound was determined by cavity ring-down spectroscopy, which allowed for highly sensitive measurements of the UV absorption bands.<sup>231</sup> The obtained barrier heights in the ground state were ca. 2.7 kJ/mol for the two modes of rotation, namely, symmetric and antisymmetric normal mode twists (Figure 44). These barriers are comparable to the experimental and theoretical values for DPE in Table 2. The electronic spectra of *p*PPE oligomers up to the decamer were studied by theoretical calculations.<sup>232</sup> Molecular orbital analyses revealed that the extent of conjugation can be significantly reduced by conformational rotation from the fully planar conformation, leading to the blue shifts of the absorption and emission bands.

The above results show that the electronic and other properties of DPE-type molecular wires are influenced by the conformation as well as the chain length. Much effort has been exerted to control the conformation of phenylene moieties. Examples of conformationally regulated wires are shown in Figure 45. In **88**, each phenyl group has two amide moieties or two ester moieties to form a hydrogen bond network in the coplanar conformation.<sup>233</sup> The extended conjugation was confirmed on the basis of the photophysical data of the trimer, the pentamer, and the heptamer. Com-

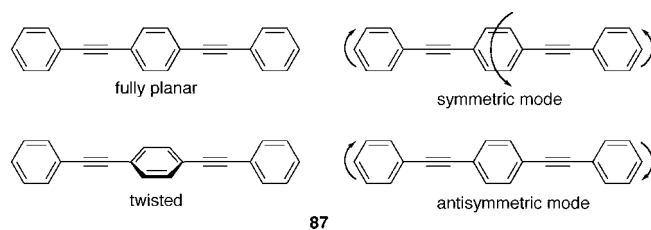


**Figure 44.** Conformation of 1,4-bis(phenylethynyl)benzene (**87**) and its rotational modes.

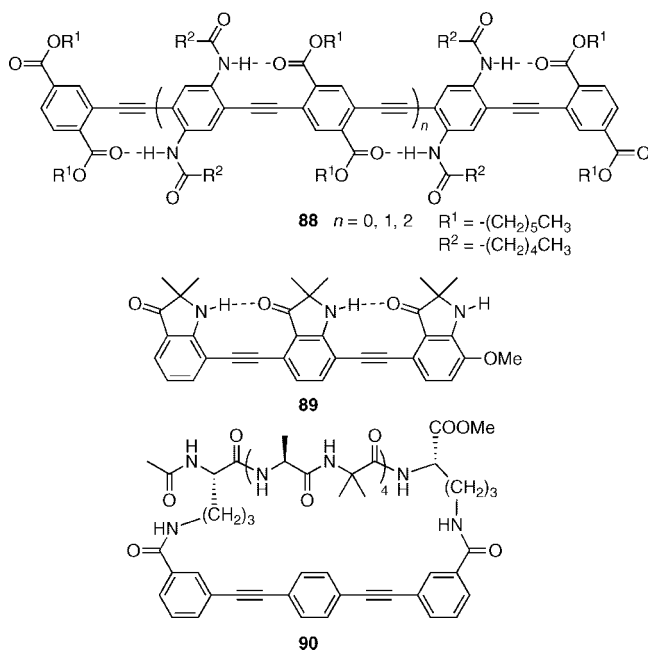


**Figure 45.** Conformationally regulated *p*-phenylene-ethynylene wires, coplanar compounds **88** and **89**, and helical compound **90**.

Compound **89** was synthesized as a mimetic of the  $\beta$ -strand in protein chemistry, where indolin-3-one moieties form successive hydrogen bond networks.<sup>234</sup> The sense of the twisted conformation is controlled by an enantiopure helical peptide bridge across the terminal phenyl groups in the trimer structure.<sup>235</sup> Compound **90** gave induced CD bands in the UV region due to the linear chain helicity. The structures of *p*PE oligomers and polymers are modified by the introduction of substituents at phenylene moieties to develop new organic materials. Swager and co-workers designed fascinating structures with various functional groups as chemical sensors and devices, where the photophysical properties of the *p*PE chromophores are sensitively influenced by the environment involving conformation.<sup>236–238</sup> In their models, triptycene and pentyptycene units are occasionally adopted as arene units to control the molecular arrangement and the fluorescence performance.

There are a large number of molecular wires consisting of other aromatic units, such as polycyclic and heterocyclic aromatic units,<sup>3,229,238,239</sup> and only a few examples are introduced here. Di-9-anthrylethyne is a repeating unit of molecular wires with anthracene rings and takes a planar conformation to maximize the stabilization by conjugation,<sup>240</sup> regardless of a low barrier to rotation about the acetylene axis. The electronic properties of trimer **91**<sup>241</sup> and the magnetic character of **92** with pendant radicals and its longer analogues<sup>242,243</sup> are well deduced from the planar conformations (Figure 46). Another type of wirelike molecule is the 1,5-naphthylene-ethynylene oligomer, although the main chains are not always rigid and linear.<sup>244,245</sup> According to the structural analysis of model compounds such as di-1-naphthylbutadiyne, all aromatic moieties in **93** and **94** prefer to take the *ap* conformation about the linkers to form zigzag chains. Porphyrin cores are also intriguing aromatic units in molecular wires.<sup>204</sup> One of the longest well-defined oligomers is hexamer **95** ( $n = 6$ ) with ca. 8 nm length.<sup>246</sup> In this series of compounds, the Q-band absorptions are red-shifted ( $\lambda$  630  $\rightarrow$  820 nm) with increasing chain length ( $n = 1 \rightarrow 6$ ),

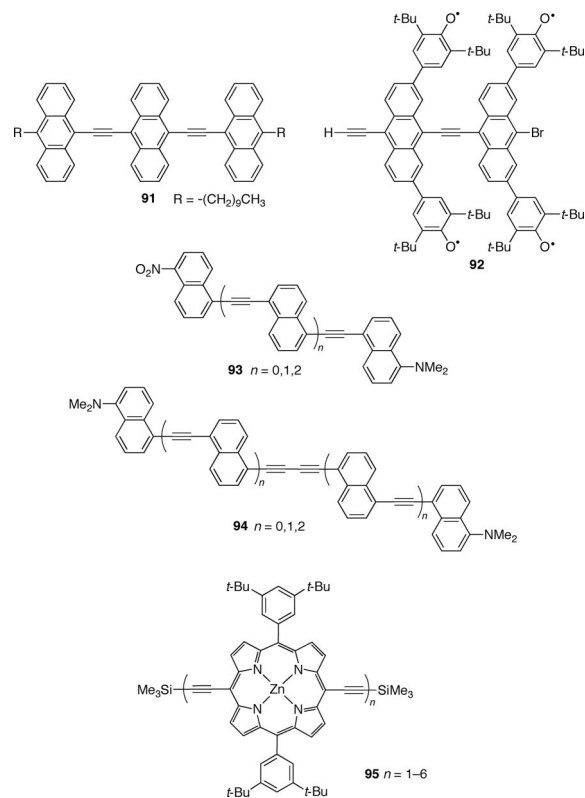


**Figure 46.** Molecular wires and related nanostructures with arene and porphyrin units.

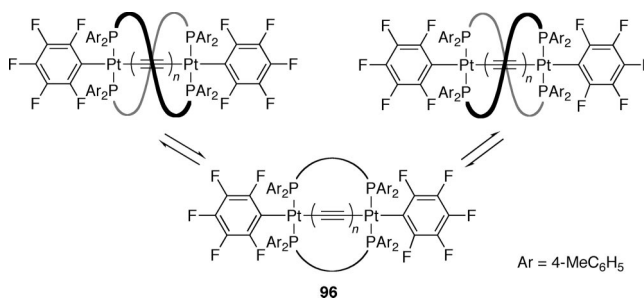


**Figure 47.** Interconversion between two chiral forms of diplatinum polyynes **96**. Polymethylene  $-(CH_2)_m-$  chains are abbreviated as curved lines.

although the rotation about butadiyne linkers may take place very rapidly in solution.

Platinum complexes **96** are also regarded as extended biphenyls (Figure 47).<sup>247</sup> In this case, two square planar Pt atoms are involved in the linker moiety. When the terminal platinum atoms are spanned with two diphenylphosphine ligands, the relative conformation between the terminal groups and the dynamic properties are influenced by the chain lengths of the polyynyl and ligand moieties.<sup>248</sup> In **96** ( $m = 14$ ,  $n = 3$ ), the alkyl chains twist around the  $C_6$  wire in a chiral double-helical structure, and this molecule undergoes rapid interconversion between helical enantiomers in solution at low temperature. In contrast, analogous complex **96** ( $m = 8$ ,  $n = 2$ ) with  $C_8$  chains and  $C_4$  wire takes a nonhelical conformation, undergoing interconversion between the two stereoisomers at a rotational barrier of 33 kJ/mol.

### 6.3. Molecular Scaffolds

The structural features of acetylene and related linear linkers are utilized to construct molecular scaffolds and

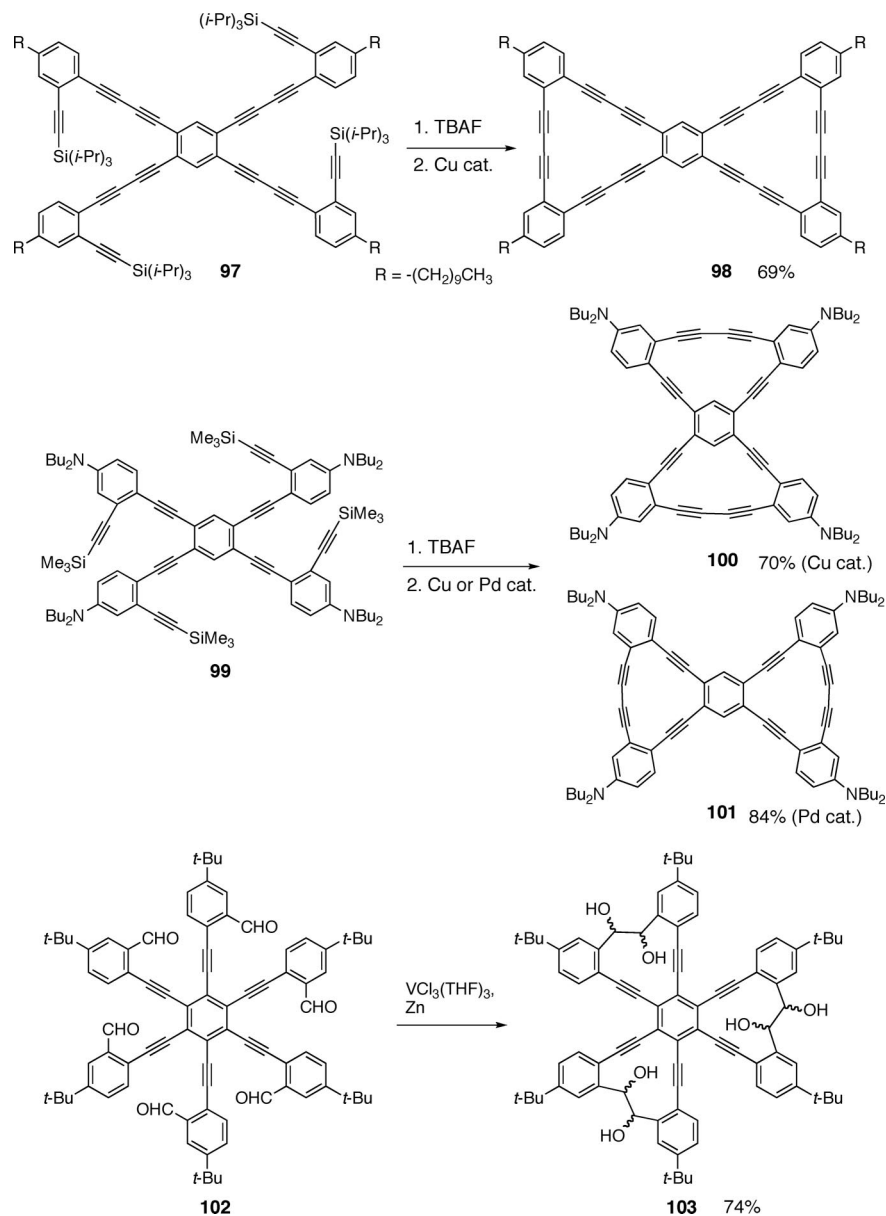


**Figure 48.** Conformationally directed macrocyclization to form multiple cyclic systems.

control the alignment of constituent units. Although we have already seen several such examples above, some additional compounds involving dendrimers and oligomers are introduced here.

The conformational characteristics of macrocyclic compounds based on phenylene units and acetylene or longer linkers have been discussed in section 5.1.4. Most of these compounds were synthesized by the metal-catalyzed macrocyclization of acyclic precursors,<sup>249,250</sup> where the linearly rigid but rotatable nature of the acetylene axis was an important factor for the effective synthesis. For example, although the terminal alkyne moieties should be randomly oriented in the desilylated product of **97**, the rotation about the diacetylene linkers directs intramolecular coupling to form doubly cyclized product **98** in high yield (Figure 48).<sup>251</sup> Interestingly, coupling of the terminal alkyne derived from **99** gave different products **100** and **101** depending on the metal catalyst.<sup>252</sup> This selectivity can be explained by the formation of different metal-acetylide intermediates due to facile rotation about the four acetylene axes. The cyclization of **102** by pinacol coupling is also accompanied by rotation

about the six acetylene axes to form tricyclic product **103** in a reasonable yield regardless of the possibility of site-random coupling.<sup>253</sup> The vicinal diol moieties can be transformed into triple bonds by a conventional method.

Several types of structures are constructed with acetylene linkers as shown in Figure 49. For example, 1,8-diethynylanthracene units can furnish cyclic structure **104** having a hexagonal prism shape by incorporating *m*-terphenyl units.<sup>254</sup> This system is proposed to form two-dimensional polymers by the intermolecular photodimerization of the anthracene moieties. In **105**, benzene rings in *p*-cyclophane moieties and terminal anthracene groups are layered with 4,5-diethynyl-9,9-dimethylxanthene units in polymeric chains.<sup>255</sup> Compound **106** is an example of arylene-ethynylene polymers involving enantiopure arene units.<sup>256,257</sup> This material is expected to have chiral configurations, even though the linker moieties can rotate within a certain range.

Acetylene linkers are also utilized in extending the structures of branched molecules such as dendrimers.<sup>258</sup> Compound **107** is a propeller-shaped molecule with three doubly branched arms bearing hydrophilic substituents



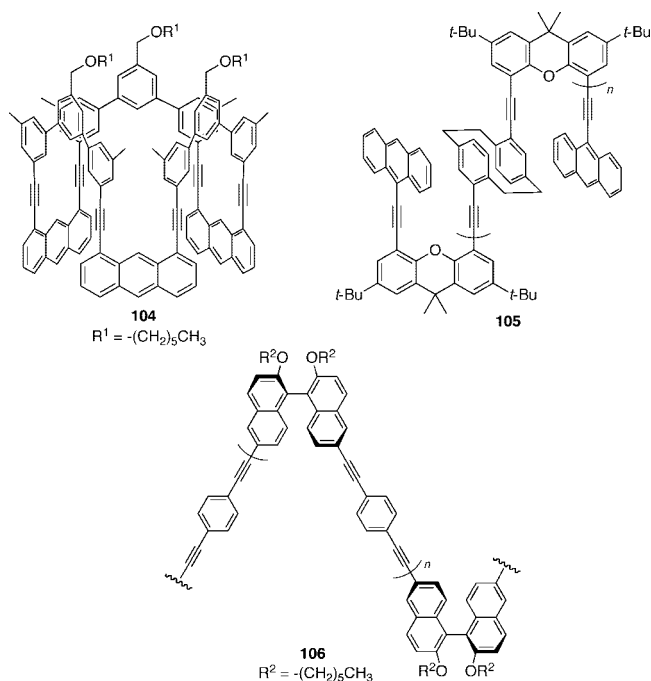


**Figure 49.** Application of acetylene linkers in cyclic and acyclic scaffolds.

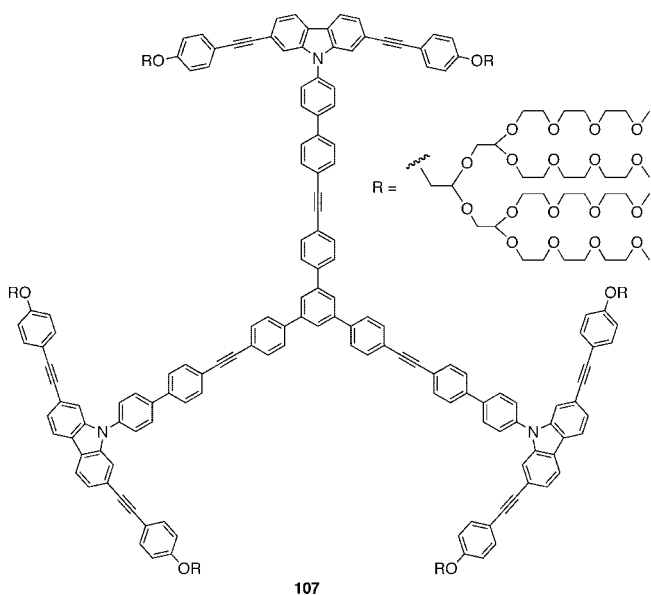


**Figure 50.** Propeller-shaped branched aromatic compound with hydrophilic chains.

(Figure 50).<sup>259</sup> The molecules are self-assembled into a well-defined structure in the water–THF system, and this unique aggregation behavior is attributed to the conformationally flexible aromatic cores. Moore and his co-workers reported several types of dendrimers and related compounds with DPE repeating units.<sup>260</sup> Compound **108** is an example of dendrons with seven phenyl groups, and this molecule can take a coplanar or twisted form (Figure 51).<sup>261</sup> This precursor was convergently extended to form dendrimer **109** with 94 benzene rings, which possessed a globular shape with ca. 55 Å diameter to avoid steric interactions by twisting about each linker. When longer DPE linkers are incorporated into the central region, larger dendrimers of up to 127-mer can be built.<sup>262</sup> Thus, the shape of branched molecules depends on the generation, the number of branches, the length of linker moieties, and other conditions.

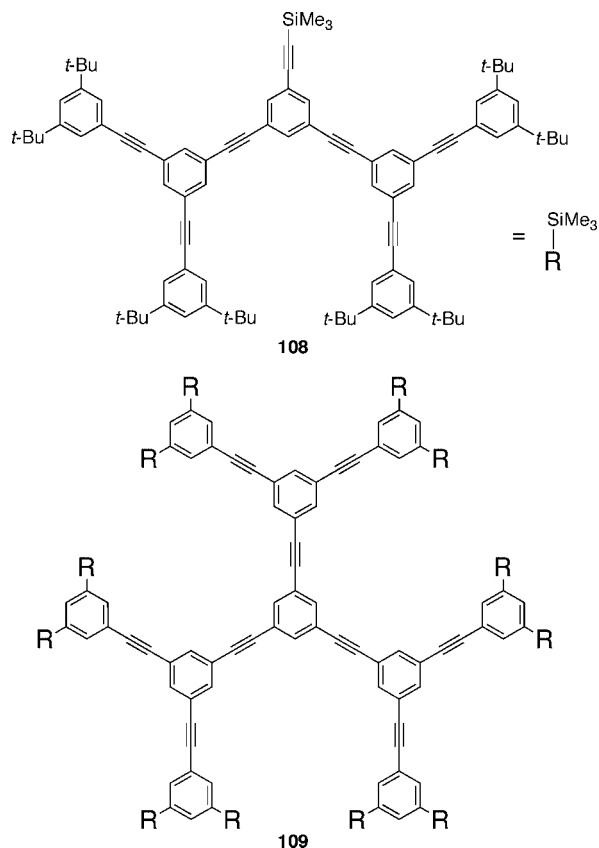


**Figure 51.** Dendron **108** and dendrimer **109** composed of DPE repeating units.

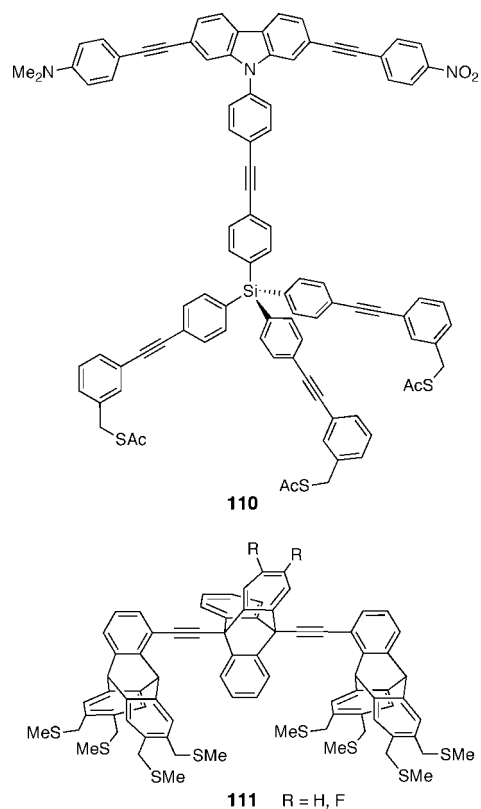


**Figure 52.** Molecular rotors with sulfur functionalities for mounting on a gold surface.

Figure 52 shows examples of molecular motors with sulfur functionalities as stator mounted on a gold surface. Compound **110** possesses a tripod base, and the carbazole-based

arms can rotate relative to the base moiety about the acetylene axis.<sup>263</sup> Donor–acceptor groups are introduced in the arm moiety for an attempt at controlling its rotation in response to the outer electric field. Compounds **111**, possessing three triptycene groups and two acetylene linkers, were designed to realize a molecular altitudinal rotor.<sup>163</sup> If eight sulfur atoms in the 1-triptycyl stands are tightly bonded to the gold surface, the central triptycene paddle can rotate about the acetylene axis.

## 6.4. Molecular Recognition

The rotation about the acetylene axis plays important roles in molecular recognition. In typical cases, host molecules carry multiple binding sites via acetylene linkers and readily change their shapes by rotation in order to fit guest molecules. These phenomena involving preorganization, cooperativity, selectivity, and chelate effects are detectable by spectroscopic measurement and occasionally by visual observation. Only selected examples of such systems are introduced here.

Extended hexaphenylethane derivative **112** carries a coordination site at each phenyl group (Figure 53).<sup>264</sup> Once the first equivalent of Ag(I) ion is captured by coordination sites across the acetylene axis, the resulting conformational change from the staggered form to the nearly eclipsed one considerably accelerates the binding of additional equivalents of Ag(I) ions. This cooperative effect can be monitored by fluorescence measurement. This strategy was applied to other extended hexaphenylethanes with longer linkers, diyne and phenylenediyne, to monitor metal and dicarboxylate ions by fluorescence measurement.<sup>265,266</sup> Compound **113** was originally designed by Kelly as a molecular brake with a 9-triptycyl group and a bipyridine unit (Figure 54).<sup>267</sup> The coordination of this bidentate ligand to a metal ion results in a conformational change so that the fused naphtho moiety is directed into a notch of the triptycene unit. However, NMR spectroscopy revealed no restricted rotation upon the addition of a metal ion because of facile rotation. This function was realized by using a nonextended system without an acetylene linker.<sup>268</sup>

Compound **114** was designed for the molecular recognition of the clinical anticoagulant heparin by incorporation of phenylboronic acids and ammonium groups into a 1,3,5-tris(phenylethynyl)benzene core (Figure 55).<sup>269</sup> The three side chains can come to the same side of the central benzene core by rotation about the acetylene axis, which results in high selectivity and affinity for various types of heparin. Compound **115** also has a similar trefoil structure with three chlorophyll units and forms a 3:3 supramolecular system with DABCO.<sup>270</sup> Bis-porphyrin tweezer host **116** forms complexes with pyridine, 4,4'-bipyridine, and other bidentate ligands.<sup>271,272</sup> The cavity size, which is defined by the distance between the two Zn atoms, is adjustable by rotation about the acetylene and diacetylene linkers.

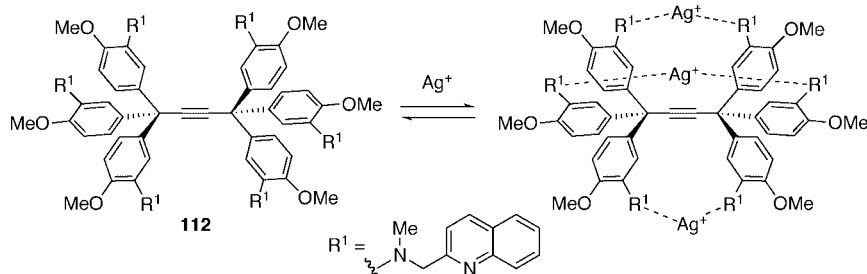


**Figure 53.** Cooperative complexation of extended hexaphenylethane with six coordination sites.

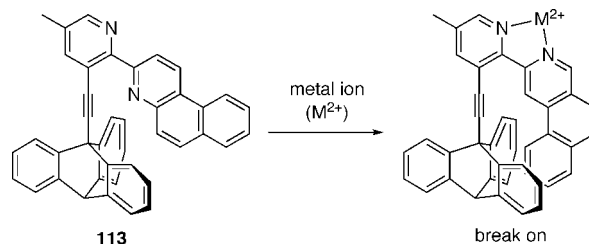


**Figure 54.** Original model of molecular brake by using metal coordination.

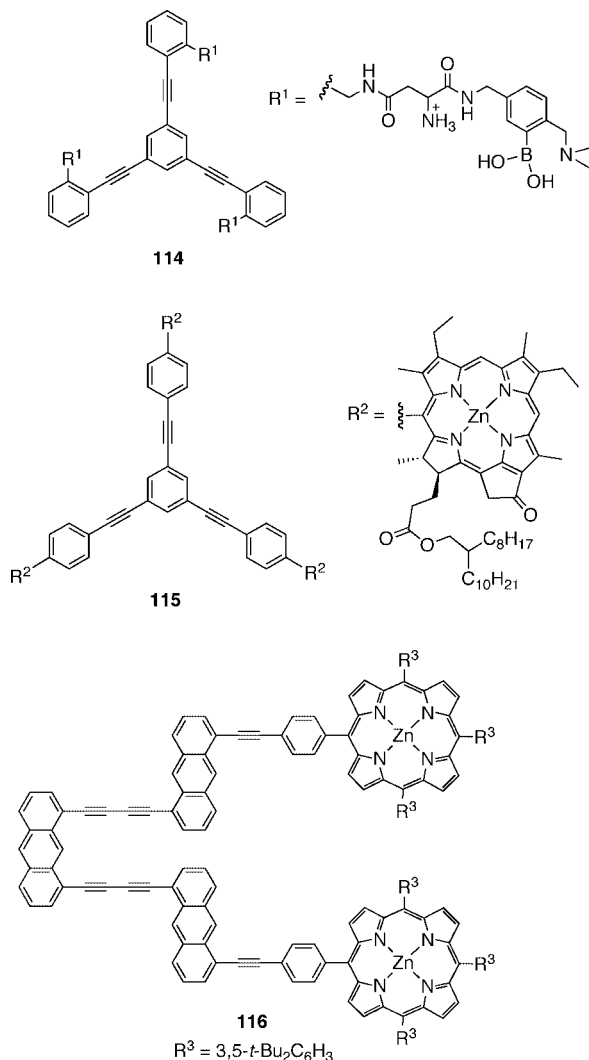


**Figure 55.** Typical examples of host compounds with acetylene linkers and multiple binding sites.

## 7. Conclusions and Perspectives

In the early days following the discovery of the rotation about the acetylene axis as a meaningful phenomenon in

structural chemistry 70 years ago, studies of rotational isomerism involving the acetylene axis had been conducted constantly but slowly because of limitations in the methods available for the observation of small energy processes. Nevertheless, research in this field has grown rapidly in the last 30 years, owing to the rapid development of experimental and theoretical methodologies. Recent widespread studies have been sparked by the application of a great number of alkynes of small to ultralarge sizes to supramolecules and functional molecules, accompanied by innovations in alkyne synthesis.

As described in the previous sections, acetylene and related linkers are unique building blocks that can connect two units in a linear fashion and potentially extend conjugation through their  $\pi$  electrons. The rotational isomerism about such long axes can be discussed on the basis of the well-established concept for ordinary single bonds, although the rotational barriers are very low in the extended system. The observed and calculated data suggested that the barrier heights were influenced by electronic effects, steric effects, weak interactions, and other factors, some of which were only recently revealed by modern techniques. The rotational barriers can be controlled by modifying the original structures of the extended ethane and biphenyl. The rotation can be restricted in sterically hindered alkynes by steric effects, leading to a few examples of rotational isomers isolable at room temperature. On the other hand, a molecular design was proposed to enhance the rotation rate of rotor moieties in the solid state, as exemplified by molecular gyroscopes. Some acyclic arylene–ethynylene oligomers form helical structures in appropriate solvent systems, producing interesting properties in the chemistry of helicates. Diarylethyne and their extended derivatives are chromophores that show characteristic absorption and emission bands in electronic spectra, and their performances are influenced by the conformation of aryl moieties about the acetylene axis. These structural and spectroscopic properties are applied to the construction of large systems such as molecular vehicles, dendrimers, and molecular wires. Acetylene units are occasionally used as linkers to maintain an appropriate distance between two terminal groups with easy rotation about the axis. This feature is available in preorganizing recognition sites in supramolecular systems, resulting in molecular sensors, switches, and other devices.

The above findings show that the rotational isomerism about the acetylene axis is an important topic in organic stereochemistry and has spread over interdisciplinary fields of material and biological sciences. The versatility of acetylene units as linkers is due to the linear connections at adjustable lengths as well as the ease of connection by various synthetic approaches toward acetylene formation or coupling. Therefore, it is possible to introduce long branches or arms into a core structure by using acetylene linkers, in which the rotation about the long axes can result in a dramatic change in the molecular structure. Recently, long polyynes, up to decaynes and beyond, have become accessible by modern synthetic techniques.<sup>32,33</sup> It is interesting to see to what extent the conformational change is observable across a linear axis (e.g., 2.8 nm for a linear decayne across 21 bonds). One of the possible ways to determine the conformation of such long alkynes is STM or related microscopic measurements on surfaces. The conformation of alkynes should influence their reactivity, but the effects have not been well noticed so far. If there are differences in rates and

selectivity of the reactions of alkyne conformers, one can observe stereoselectivity in alkyne chemistry, which is a novel phenomenon in terms of the remote control of reactions across a long axis. Studies on the control of rotational barriers in various alkynes are underway, and great progress is expected. The further enhancement of rotational barriers in acyclic alkynes would lead to the isolation of rotational isomers, namely atropisomers, at room temperature, which would make it possible to investigate the properties and reactivities of each isomer separately. The dynamic behavior of acetylene rotation in the solid state is an attractive phenomenon to realize facile or correlated rotation toward real molecular gears and gyroscopes in the crystal lattice. These subjects should be tackled by chemists in the future to magnify the importance of the stereochemical aspect in alkyne chemistry.

## 8. Acknowledgments

The author thanks Professor Emeritus Michinori Ōki for valuable advice and continuous encouragement. The author also thanks Dr. Tetsuo Iwanaga and Professor Kan Wakamatsu for helpful assistance and discussions.

## 9. Note Added in Proof

A macrocyclic arylene–ethynylene oligomer with anthracene and pyridine units was synthesized as a shape-persistent cyclic arylythyne.<sup>273</sup> Molecular hinge **68** with triphenylene units instead of pyrene units was found to form intramolecular excimer in the excited state.<sup>274</sup> A new highly fluorescent nanocar with *p*-carborane wheels was reported.<sup>275</sup>

## 10. References

- (1) Moss, G. P. *Pure Appl. Chem.* **1996**, *68*, 2193.
- (2) Eliel, E. L.; Wilen, S. H.; Mander, L. N. *Stereochemistry of Organic Compounds*; John Wiley & Sons, Inc.: New York, 1994; p 627.
- (3) *Poly(arylene ethynylene)s*; Weder, C., Ed.; Springer: Berlin, 2005.
- (4) Lukas, A. S.; Wasielewski, M. R. *Molecular Switches*; Wiley-VCH: Weinheim, 2001; Chapter 1.
- (5) Houk, K. N.; Scott, L. T.; Rondan, N. G.; Spellmeyer, D. C.; Reinhardt, G.; Hyun, J. L.; DeCicco, G. J.; Weiss, R.; Chen, M. H. M.; Bass, L. S.; Clardy, J.; Jorgensen, F. S.; Saton, T. A.; Sarkozi, V.; Petit, C. M.; Ng, L.; Jordan, K. D. *J. Am. Chem. Soc.* **1985**, *107*, 6556.
- (6) Maraval, V.; Chauvin, R. *Chem. Rev.* **2006**, *106*, 5317.
- (7) Maraval, V.; Chauvin, R. *New J. Chem.* **2007**, *31*, 1853.
- (8) Young, J. K.; Moore, J. S. In *Modern Acetylene Chemistry*; Stang, P. J., Diederich, F., Eds.; VCH: Weinheim, 1995; Chapter 12.
- (9) Balzani, V.; Venturi, M.; Credi, A. *Molecular Devices and Machines*; Wiley-VCH: Weinheim, 2003.
- (10) Kottas, G. S.; Clarke, L. I.; Horinek, D.; Michl, J. *Chem. Rev.* **2005**, *105*, 1281.
- (11) Brandsma, L. *Synthesis of Acetylenes, Allenes and Cumulenes*; Elsevier: Oxford, 2004.
- (12) *Polyynes, Arynes, Enynes, and Alkynes*; Science of Synthesis Vol. 43; Hopf, H., Ed.; Thieme: Stuttgart, 2008; Chapters 43.6–43.8.
- (13) Chinchilla, R.; Nájera, C. *Chem. Rev.* **2007**, *107*, 874.
- (14) Sonogashira, K. In *Handbook of Organopalladium Chemistry for Organic Synthesis*; Negishi, E.-i., de Meijere, A., Eds.; John Wiley & Sons, Inc.: New York, 2002; Vol. 1, p 493.
- (15) Bunz, U. H. F. In *Modern Arene Chemistry*; Astruc, D., Ed.; Wiley-VCH: Weinheim, 2002; Chapter 7.
- (16) Zhang, W.; Moore, J. S. *Adv. Synth. Catal.* **2007**, *349*, 93.
- (17) Otera, J. *Pure Appl. Chem.* **2006**, *78*, 731.
- (18) Orita, A.; Otera, J. *Chem. Rev.* **2006**, *106*, 5387.
- (19) Zanatta, S. D. *Aust. J. Chem.* **2007**, *60*, 963.
- (20) Eymery, F.; Iorga, B.; Savignac, P. *Synthesis* **2000**, 185.
- (21) Kirmse, W. *Angew. Chem., Int. Ed.* **1997**, *36*, 1164.
- (22) Eymery, F.; Iorga, B.; Savignac, P. *Synthesis* **2000**, 185.
- (23) *Acetylene Chemistry*; Diederich, F., Stang, J. J., Tykwinski, R. R., Eds.; Wiley-VCH: Weinheim, 2005.



- (24) *Carbon-Rich Compounds*; Haley, M. M., Tykwinski, R. R., Eds.; Wiley-VCH: Weinheim, 2006.
- (25) Reference 2, Chapter 10.
- (26) Klyne, W.; Prelog, V. *Experientia* **1960**, *16*, 521.
- (27) Lister, D. G.; Macdonald, J. N.; Owen, N. L. *Internal Rotation and Inversion*; Academic Press: London, 1978; Chapter 2.
- (28) Gleiter, R.; Merger, R. Reference 8, Chapter 8.
- (29) Eisler, S.; McDonald, R.; Loppnow, G. R.; Tykwinski, R. R. *J. Am. Chem. Soc.* **2000**, *122*, 6917.
- (30) de Graaff, R. A. G.; Gorter, S.; Romers, C.; Wong, H. N. C.; Sondheimer, F. *J. Chem. Soc., Perkin Trans. 2* **1981**, 478.
- (31) Gleiter, R.; Kratz, D.; Schäfer, W.; Schehlmann, V. *J. Am. Chem. Soc.* **1991**, *113*, 9258.
- (32) Eisler, S.; Slepko, A. D.; Elliott, E.; Luu, T.; McDonald, R.; Hegmann, F. A.; Tykwinski, R. R. *J. Am. Chem. Soc.* **2005**, *127*, 2666.
- (33) Lucotti, A.; Tommasini, M.; Fazzi, D.; Zoppo, M. D.; Chalifoux, W. A.; Ferguson, M. J.; Zerbi, G.; Tykwinski, R. R. *J. Am. Chem. Soc.* **2009**, *131*, 4239.
- (34) Dodziuk, H. *Modern Conformational Analysis*; VCH: New York, 1995; Chapters 2 and 3.
- (35) Ōki, M. *Applications of Dynamic NMR Spectroscopy to Organic Chemistry*; VCH: Deerfield Beach, 1985.
- (36) Schaefer, T.; Sebastian, R.; Schurko, R. W. *Can. J. Chem.* **1992**, *70*, 2365.
- (37) Alkorta, I.; Elguero, J. *Org. Biomol. Chem.* **2003**, *1*, 585.
- (38) Crawford, B. R., Jr.; Rice, W. W. *J. Chem. Phys.* **1939**, *7*, 437.
- (39) Osborne, D. W.; Garner, C. S.; Yost, D. M. *J. Chem. Phys.* **1940**, *8*, 131.
- (40) Mills, I. M.; Thompson, H. W. *Proc. R. Soc. London, Ser. A: Math. Phys. Sci.* **1954**, *226*, 306.
- (41) Langseth, A.; Bernstein, H. J.; Bak, B. *J. Chem. Phys.* **1940**, *8*, 415.
- (42) Lassetre, E.; Dean, L. B., Jr. *J. Chem. Phys.* **1949**, *17*, 317.
- (43) Mason, E. A.; Kreevoy, M. M. *J. Am. Chem. Soc.* **1955**, *77*, 5808.
- (44) Kirtman, B. *J. Chem. Phys.* **1964**, *41*, 775.
- (45) Kopelman, R. *J. Chem. Phys.* **1964**, *41*, 1547.
- (46) Olson, W. B.; Papousek, D. *J. Mol. Spectrosc.* **1971**, *37*, 527.
- (47) Nakagawa, J.; Hayashi, M.; Endo, Y.; Saito, S.; Hirota, E. *J. Chem. Phys.* **1984**, *80*, 5922.
- (48) Bunker, P. R.; Johns, J. W. C.; McKellar, A. R. W.; Di Lauro, C. J. *Mol. Spectrosc.* **1993**, *162*, 142.
- (49) Plíva, J.; Pine, A. S.; Civiš, S. *J. Mol. Spectrosc.* **1996**, *180*, 15.
- (50) Ibberson, R. M.; Prager, M. *Acta Crystallogr.* **1995**, *B51*, 71.
- (51) Radom, L.; Pople, J. A. *J. Am. Chem. Soc.* **1970**, *92*, 4786.
- (52) Kollman, P. A.; Bender, C. F.; McKelvey, J. *J. Chem. Phys. Lett.* **1974**, *28*, 407.
- (53) Radom, L.; Stiles, P. J.; Vincent, M. A. *J. Mol. Struct.* **1978**, *48*, 259.
- (54) Frolov, Yu. L.; Knizhnik, A. V. *J. Struct. Chem.* **2002**, *43*, 856.
- (55) Goldstein, E.; Ma, B.; Lii, J.-H.; Allinger, N. L. *J. Phys. Org. Chem.* **1996**, *9*, 191.
- (56) Goodman, L.; Pophristic, V.; Weinhold, F. *Acc. Chem. Res.* **1999**, *32*, 983. Mo, Y.; Gao, J. *Acc. Chem. Res.* **2007**, *40*, 113; see also references therein.
- (57) Thomas, R.; Lakshmi, S.; Pati, S. K.; Kulkarni, G. U. *J. Phys. Chem. B* **2006**, *110*, 24674.
- (58) Abramov, A. V.; Almenningen, A.; Cyvin, B. N.; Cyvin, S. J.; Jonvik, T.; Khaikin, L. S.; Romming, C.; Vilkov, L. V. *Acta Chim. Scand.* **1988**, *A42*, 674.
- (59) Mavridis, A.; Moustakali-Mavridis, I. *Acta Crystallogr.* **1977**, *B33*, 3612.
- (60) Desiraju, G. R.; Krishna, T. S. R. *J. Chem. Soc., Chem. Commun.* **1988**, 192.
- (61) Okuyama, K.; Hasegawa, T.; Ito, M.; Mikami, N. *J. Phys. Chem.* **1984**, *88*, 1711.
- (62) Grumadas, A. Yu.; Poshkus, D. P. *Russ. J. Phys. Chem.* **1987**, *61*, 1495.
- (63) Liberles, A.; Matlosz, B. *J. Org. Chem.* **1971**, *36*, 2710.
- (64) Li, Y.; Zhao, J.; Yin, X.; Yin, G. *ChemPhysChem* **2006**, *7*, 2593.
- (65) Shimojima, A.; Takahashi, H. *J. Phys. Chem.* **1993**, *97*, 9103.
- (66) Saebo, S.; Almlöf, J.; Boggs, J.; Stark, J. G. *THEOCHEM* **1989**, *200*, 361.
- (67) Seminario, J.; Zacarias, A. G.; Tour, J. M. *J. Am. Chem. Soc.* **1998**, *120*, 3970.
- (68) Li, Y.; Zhao, J.; Yin, X.; Liu, H.; Yin, G. *J. Phys. Chem. Chem. Phys.* **2007**, *9*, 1186.
- (69) Brizius, G.; Billingsley, K.; Smith, M. D.; Bunz, U. H. F. *Org. Lett.* **2003**, *5*, 3951.
- (70) Reference 2, Chapter 14.5.
- (71) Johansson, M. P.; Olsen, J. *J. Chem. Theory Comput.* **2008**, *4*, 1460. Tsuzuki, S.; Tanabe, K. *J. Phys. Chem.* **1991**, *95*, 139; see also references therein.
- (72) Almenningen, A.; Gogstad, E.; Hagen, K.; Schei, H.; Stølevik, R.; Thingstad, Ø.; Traetteberg, M. *J. Mol. Spectrosc.* **1984**, *116*, 131.
- (73) Tørnøng, E.; Nielsen, C. J.; Klæboe, P.; Hopf, H.; Schüll, V. *J. Mol. Spectrosc.* **1981**, *71*, 71.
- (74) Frolov, Yu. L.; Knizhnik, A. V.; Chipanina, N. N. *J. Struct. Chem.* **1997**, *38*, 163.
- (75) Frolov, Yu. L.; Knizhnik, A. V. *J. Struct. Chem.* **1998**, *39*, 496.
- (76) Knizhnik, A. V.; Frolov, Yu. L. *J. Struct. Chem.* **2002**, *43*, 41.
- (77) Reference 2, Chapter 10.2.
- (78) Jarowski, P. D.; Diederich, F.; Houk, K. N. *J. Phys. Chem. A* **2006**, *110*, 7237.
- (79) Murcko, M. A.; Castejon, H.; Wiberg, K. B. *J. Phys. Chem.* **1996**, *100*, 16162.
- (80) Carey, F. A.; Sundberg, R. J. *Advanced Organic Chemistry*, 4th ed., Part A; Kluwer Academic/Plenum Publisher: New York, 2000; Chapter 4.
- (81) Anslyn, E. V.; Dougherty, D. A. *Modern Physical Organic Chemistry*; University Science Books: Sausalito, 2006; Chapter 8.2.
- (82) Bohn, R. K. *J. Phys. Chem. A* **2004**, *108*, 6814.
- (83) Churchill, G. B.; Bohn, R. K. *J. Phys. Chem. A* **2007**, *111*, 6814.
- (84) Stølvijk, V. M.; van Eijck, B. P. *J. Mol. Spectrosc.* **1987**, *124*, 92.
- (85) Laurie, V. W.; Lide, D. R., Jr. *J. Chem. Phys.* **1959**, *31*, 939.
- (86) Fournier, J. A.; Bohn, R. K.; Michels, H. H. *J. Mol. Spectrosc.* **2008**, *251*, 145.
- (87) Subramanian, R.; Novick, S. E.; Bohn, R. K. *J. Mol. Spectrosc.* **2003**, *222*, 57.
- (88) Blanco, S.; Sanz, M. E.; Lesarri, A.; López, J. C.; Alonso, J. L. *Chem. Phys. Lett.* **2004**, *397*, 379.
- (89) Ohashi, S.; Inagaki, S. *Tetrahedron* **2001**, *57*, 5361.
- (90) Radom, L.; Vincent, M. A. *Isr. J. Chem.* **1980**, *19*, 305.
- (91) Hensel, K. D.; Gerry, M. C. L. *J. Chem. Soc., Faraday Trans.* **1994**, *90*, 3023.
- (92) Nakagawa, J.; Yamada, K.; Bester, M.; Winnewisser, G. *J. Mol. Spectrosc.* **1985**, *110*, 74.
- (93) Sipachev, V. A.; Khaikin, L. S.; Grikin, O. E.; Nikitin, V. S.; Trætteberg, M. *J. Mol. Struct.* **2000**, *523*, 1.
- (94) Chalifoux, W. A.; Tykwinski, R. R. *C. R. Chim.* **2009**, *12*, 341.
- (95) Eisler, S.; Tykwinski, R. R. Reference 23, Chapter 7.
- (96) Yam, V. W. W.; Tao, C. H. Reference 24, Chapter 10.
- (97) Nielsen, C. J. *Spectrochim. Acta, A* **1983**, *39*, 993.
- (98) Nakovich, J., Jr.; Shook, S. D.; Miller, F. A.; Parmell, D. R.; Sacher, R. E. *Spectrochim. Acta, A* **1979**, *35*, 495.
- (99) Baranović, G.; Colombo, L.; Furić, K.; Durig, J. R.; Sullivan, J. F.; Mink, J. *J. Mol. Struct.* **1986**, *144*, 53.
- (100) Stølevik, R.; Bakken, P. *J. Mol. Struct.* **1990**, *239*, 205.
- (101) Iwamura, H.; Mislow, K. *Acc. Chem. Res.* **1988**, *21*, 175.
- (102) Stevens, A. M.; Richards, C. J. *Tetrahedron Lett.* **1997**, *38*, 7805.
- (103) Yang, X.; Brown, A. L.; Furukawa, M.; Li, S.; Gardinier, W. E.; Bukowski, E. J.; Bright, F. V.; Zheng, C.; Zeng, X. C.; Gong, B. *Chem. Commun.* **2003**, 56.
- (104) Yang, X.; Yuan, L.; Yamato, J.; Brown, A. L.; Feng, W.; Furukawa, M.; Zeng, X. C.; Gong, B. *J. Am. Chem. Soc.* **2004**, *126*, 3148.
- (105) Kemp, D. S.; Li, Z. Q. *Tetrahedron Lett.* **1995**, *36*, 4175.
- (106) Reichardt, C. *Solvents and Solvent Effects in Organic Chemistry*, 3rd ed.; Wiley-VCH: Weinheim, 2003; Chapter 2.
- (107) Zhao, Y.; Moore, J. S. In *Foldamers*; Hecht, S., Huc, I., Eds.; Wiley-VCH: Weinheim, 2007; Chapter 3.
- (108) Inoue, K.; Takeuchi, H.; Konaka, S. *J. Phys. Chem. A* **2001**, *105*, 6711.
- (109) Takeuchi, H. *Ekisho* **2002**, *6*, 383.
- (110) Albert, S.; Ripmeester, J. A. *J. Chem. Phys.* **1972**, *57*, 5336.
- (111) Alefeld, B.; Kollmar, A. *Phys. Lett.* **1976**, *57A*, 289.
- (112) Tilli, K. J.; Alefeld, B. *Mol. Phys.* **1978**, *36*, 287.
- (113) Kristein, O.; Prager, M.; Johnson, M. R.; Parker, S. F. *J. Chem. Phys.* **2002**, *117*, 1313.
- (114) Batley, M.; Thomas, R. K.; Heidemann, A.; Overs, A. H.; White, J. W. *Mol. Phys.* **1977**, *34*, 1771.
- (115) Gutmann, M.; Gudipati, M.; Schönzart, P.-F.; Hohlneicher, G. *J. Phys. Chem.* **1992**, *96*, 2433.
- (116) Molnár, F.; Dick, B. *Ber. Bunsen-Ges. Phys. Chem.* **1995**, *99*, 422.
- (117) Hiura, H.; Takahashi, H. *J. Phys. Chem.* **1992**, *96*, 8909.
- (118) Okuyama, K.; Cockett, M. C. R.; Kimura, K. *J. Chem. Phys.* **1992**, *97*, 1649.
- (119) Toyota, S.; Iida, T.; Kunizane, C.; Tanifuji, N.; Yoshida, Y. *Org. Biomol. Chem.* **2003**, *1*, 2298.
- (120) Toyota, S.; Yanagihara, T.; Yoshida, Y.; Goichi, M. *Bull. Chem. Soc. Jpn.* **2005**, *78*, 1351.
- (121) Miljanić, O. Š.; Han, S.; Holmes, D.; Schaller, G. R.; Vollhardt, K. P. C. *Chem. Commun.* **2005**, 2606.
- (122) Toyota, S.; Makino, T. *Tetrahedron Lett.* **2003**, *44*, 7775.
- (123) Makino, T.; Toyota, S. *Bull. Chem. Soc. Jpn.* **2005**, *78*, 917.
- (124) Toyota, S.; Ebisu, N.; Makino, T. Unpublished work.



- (125) Koulotas, C.; Schwartz, L. H. *J. Chem. Soc., Chem. Commun.* **1969**, 1400.
- (126) Toyota, S.; Shimasaki, T.; Tanifuji, N.; Wakamatsu, K. *Tetrahedron: Asymmetry* **2003**, *14*, 1623.
- (127) Wilson, K. R.; Pincock, R. E. *J. Am. Chem. Soc.* **1975**, *97*, 1474.
- (128) Ōki, M. *The Chemistry of Rotational Isomers*; Springer-Verlag: Berlin, 1993; Chapter 3.3.
- (129) Schwartz, L. H.; Koulotas, C.; Kukkola, C.; Yu, C. S. *J. Org. Chem.* **1986**, *51*, 995.
- (130) Koo Tze Mew, P.; Vögtle, F. *Angew. Chem., Int. Ed.* **1979**, *18*, 159.
- (131) Toyota, S.; Yamamori, T.; Asakura, M.; Ōki, M. *Bull. Chem. Soc. Jpn.* **2000**, *73*, 205.
- (132) Toyota, S.; Yamamori, T.; Makino, T.; Ōki, M. *Bull. Chem. Soc. Jpn.* **2000**, *73*, 2591.
- (133) Toyota, S.; Yamamori, T.; Makino, T. *Tetrahedron* **2001**, *57*, 3521.
- (134) Bott, G.; Field, L. D.; Sternhell, S. *J. Am. Chem. Soc.* **1980**, *102*, 5618.
- (135) Jeffrey, G. A. *An Introduction to Hydrogen Bonding*; Oxford University Press: New York, 1997; Chapter 5.
- (136) Desiraju, G. R.; Steiner, T. *The Weak Hydrogen Bond*; Oxford University Press: New York, 1999; Chapters 2 and 3.
- (137) Werz, D. B.; Gleiter, R. *Org. Lett.* **2004**, *6*, 589.
- (138) Campbell, K.; Tykwinski, R. R. In *Carbon-Rich Compounds*; Haley, M. M., Tykwinski, R. R., Eds.; Wiley-VCH: Weinheim, 2006; Chapter 6.
- (139) Staab, H. A.; Wehinger, E.; Thorwart, W. *Chem. Ber.* **1972**, *105*, 2290.
- (140) Irrgartinger, H. *Chem. Ber.* **1973**, *106*, 761.
- (141) Boese, R.; Matzger, A. J.; Vollhardt, K. P. C. *J. Am. Chem. Soc.* **1997**, *119*, 2052.
- (142) Collins, S. K.; Yap, G. P. A.; Fallis, A. G. *Angew. Chem., Int. Ed.* **2000**, *39*, 385.
- (143) Collins, S. K.; Yap, G. P. A.; Fallis, A. G. *Org. Lett.* **2000**, *2*, 3189.
- (144) Heuft, M. A.; Collins, S. K.; Fallis, A. G. *Org. Lett.* **2003**, *5*, 1911.
- (145) Solooki, D.; Bradshaw, J. D.; Tessier, C. A.; Youngs, W. J.; See, R. F.; Churchill, M.; Ferrara, J. D. *J. Organomet. Chem.* **1994**, *470*, 231.
- (146) Baldwin, K. P.; Simons, R. S.; Rose, J.; Zimmerman, P.; Hercules, D. M.; Tessier, C. A.; Youngs, W. J. *J. Chem. Soc., Chem. Commun.* **1994**, 1257.
- (147) Utsumi, K.; Kawase, T.; Oda, M. *Chem. Lett.* **2003**, *32*, 412.
- (148) Romero, M. A.; Fallis, A. G. *Tetrahedron Lett.* **1994**, *35*, 4711.
- (149) Rubin, Y.; Parker, T. C.; Khan, S. I.; Holliman, C. L.; McElvany, S. W. *J. Am. Chem. Soc.* **1996**, *118*, 5308.
- (150) Baxter, P. N. W. *Chem.—Eur. J.* **2002**, *8*, 5250.
- (151) Heuft, M. A.; Fallis, A. G. *Angew. Chem., Int. Ed.* **2002**, *41*, 4520.
- (152) Toyota, S.; Goichi, M.; Kotani, M. *Angew. Chem., Int. Ed.* **2004**, *43*, 2248.
- (153) Toyota, S.; Goichi, M.; Kotani, M.; Takezaki, M. *Bull. Chem. Soc. Jpn.* **2005**, *78*, 2214.
- (154) Toyota, S.; Miyahara, H.; Goichi, M.; Yamasaki, S.; Iwanaga, T. *Bull. Chem. Soc. Jpn.* **2009**, *82*, 931.
- (155) Toyota, S.; Miyahara, H.; Goichi, M.; Wakamatsu, K.; Iwanaga, T. *Bull. Chem. Soc. Jpn.* **2008**, *81*, 1147.
- (156) Toyota, S.; Miyahara, H.; Harada, H. Unpublished results.
- (157) Takahira, Y.; Sugiura, H.; Yamaguchi, M. *J. Org. Chem.* **2006**, *71*, 763.
- (158) Ishikawa, T.; Shimasaki, T.; Akashi, H.; Toyota, S. *Org. Lett.* **2008**, *10*, 417.
- (159) Ishikawa, T.; Shimasaki, T.; Akashi, H.; Iwanaga, T.; Toyota, S.; Yamasaki, M. *Bull. Chem. Soc. Jpn.* **2010**, *83*, 220.
- (160) Bedard, T. C.; Moore, J. S. *J. Am. Chem. Soc.* **1995**, *117*, 10662.
- (161) Ohkita, M.; Ando, K.; Suzuki, T.; Tsuji, T. *J. Org. Chem.* **2000**, *65*, 4385.
- (162) Miyamoto, K.; Iwanaga, T.; Toyota, S. *Chem. Lett.* **2010**, *39*, 299.
- (163) Magnera, T. F.; Michl, J. *Top. Curr. Chem.* **2005**, *262*, 63.
- (164) Caskey, D. C.; Wang, B.; Zheng, X.; Michl, J. *Collect. Czech. Chem. Commun.* **2005**, *70*, 1970.
- (165) Kawase, T. *Synlett* **2007**, 2609.
- (166) Kawase, T.; Oda, M. *Pure Appl. Chem.* **2006**, *78*, 831.
- (167) Weng, W.; Bartik, T.; Brady, B.; Ramsden, J. A.; Arif, A. M.; Gladysz, J. A. *J. Am. Chem. Soc.* **1995**, *117*, 11922.
- (168) Karlen, S. D.; Garcia-Garibay, M. A. *Top. Curr. Chem.* **2005**, *262*, 179.
- (169) Khuong, T.-A. V.; Nuñez, J. E.; Codinez, C. E.; Garcia-Garibay, M. A. *Acc. Chem. Res.* **2006**, *29*, 413.
- (170) Dominguez, Z.; Dang, H.; Strouse, M. J.; Garcia-Garibay, M. A. *J. Am. Chem. Soc.* **2002**, *124*, 2398.
- (171) Dominguez, Z.; Dang, H.; Strouse, M. J.; Garcia-Garibay, M. A. *J. Am. Chem. Soc.* **2002**, *124*, 7719.
- (172) Khuong, T.-A. V.; Dang, H.; Jarowski, P. D.; Maverick, E. F.; Garcia-Garibay, M. A. *J. Am. Chem. Soc.* **2007**, *129*, 839.
- (173) Khuong, T. A. V.; Zepeda, G.; Ruiz, R.; Khan, S. I.; Garcia-Garibay, M. A. *Cryst. Growth Des.* **2004**, *4*, 15.
- (174) Jarowski, P. D.; Houk, K. N.; Garcia-Garibay, M. A. *J. Am. Chem. Soc.* **2007**, *129*, 3110.
- (175) Gould, S. L.; Rodriguez, R. B.; Garcia-Garibay, M. A. *Tetrahedron* **2008**, *64*, 8336.
- (176) Nuñez, J. E.; Natarajan, A.; Khan, S. I.; Garcia-Garibay, M. A. *Org. Lett.* **2007**, *9*, 3559.
- (177) Godinez, C. E.; Zepeda, G.; Garcia-Garibay, M. A. *J. Am. Chem. Soc.* **2002**, *124*, 4701.
- (178) Godinez, C. E.; Zepeda, G.; Mortko, C. J.; Dang, H.; Garcia-Garibay, M. A. *J. Org. Chem.* **2004**, *69*, 1652.
- (179) Garcia-Garibay, M. A.; Godinez, C. E. *Cryst. Growth Des.* **2009**, *9*, 3124.
- (180) Karlen, S. D.; Godinez, C. E.; Garcia-Garibay, M. A. *Org. Lett.* **2006**, *8*, 3417.
- (181) Nelson, J. C.; Saven, J. G.; Moore, J. S.; Wolynes, P. G. *Science* **1997**, *277*, 1793.
- (182) Ray, C. R.; Moore, J. S. *Adv. Polym. Sci.* **2005**, *177*, 91.
- (183) Lahiri, S.; Thompson, J. L.; Moore, J. S. *J. Am. Chem. Soc.* **2000**, *122*, 11315.
- (184) Wackerly, J. Wm.; Moore, J. S. *Macromolecules* **2006**, *39*, 7269.
- (185) Gin, M. S.; Moore, J. S. *Org. Lett.* **2000**, *2*, 135.
- (186) Brunsveld, L.; Prince, R. B.; Meijer, E. W.; Moore, J. S. *Org. Lett.* **2000**, *2*, 1515.
- (187) Stone, M. T.; Fox, J. M.; Moore, J. S. *Org. Lett.* **2004**, *6*, 3317.
- (188) Stone, M. T.; Moore, J. S. *Org. Lett.* **2004**, *4*, 469.
- (189) Prince, R. B.; Barnes, S. A.; Moore, J. S. *J. Am. Chem. Soc.* **2000**, *122*, 2758.
- (190) Tanatani, A.; Mio, M. J.; Moore, J. S. *J. Am. Chem. Soc.* **2001**, *123*, 1792.
- (191) Jones, T. V.; Slutsky, M. M.; Laos, R. L.; de Greef, T. F. A.; Tew, G. N. *J. Am. Chem. Soc.* **2006**, *127*, 17235.
- (192) Slutsky, M. M.; Phillip, J. S.; Tew, G. N. *New J. Chem.* **2008**, *32*, 670.
- (193) Jiang, J.; Slutsky, M. M.; Jones, T. V.; Tew, G. N. *New J. Chem.* **2010**, *34*, 307.
- (194) Zhu, N.; Hu, W.; Han, S.; Wang, Q.; Zhao, D. *Org. Lett.* **2008**, *10*, 4283.
- (195) Yagi, S.; Kitayama, H.; Takagishi, T. *J. Chem. Soc., Perkin Trans. 1* **2000**, 925.
- (196) Sankararaman, S.; Venkataramana, G.; Varghese, B. *J. Org. Chem.* **2008**, *73*, 2404.
- (197) Nandy, R.; Subramoni, M.; Varghese, B.; Sankararaman, S. *J. Org. Chem.* **2007**, *72*, 938.
- (198) Hanhela, P. J.; Paul, D. B. *Aust. J. Chem.* **1984**, *37*, 553.
- (199) Nakatsuji, S.; Matsuda, K.; Uesugi, Y.; Nakashima, K.; Akiyama, S.; Fabian, W. *J. Chem. Soc., Perkin Trans. 1* **1992**, 755.
- (200) Li, B.; Miao, W.; Cheng, L. *Dyes Pigm.* **1999**, *43*, 161.
- (201) Levitus, M.; Garcia-Garibay, M. A. *J. Phys. Chem. A* **2000**, *104*, 8632.
- (202) Beeby, A.; Findlay, K. S.; Goeta, A. E.; Porres, L.; Rutter, S. R.; Thompson, A. L. *Photochem. Photobiol. Sci.* **2007**, *6*, 982.
- (203) Terashima, T.; Nakashima, T.; Kawai, T. *Org. Lett.* **2007**, *9*, 4195.
- (204) Anderson, H. L. *Chem. Commun.* **1999**, 2323.
- (205) Anderson, H. L. *Inorg. Chem.* **1994**, *33*, 972.
- (206) Stranger, R.; McGrady, J. E.; Arnold, D. P.; Lane, I.; Heath, G. A. *Inorg. Chem.* **1996**, *35*, 7791.
- (207) The authors of ref 206 reported that the calculated barrier of **74** was ca. 63 kJ/mol by the DFT method. However, such a high barrier was unlikely, as pointed out in ref 209. We confirmed by modern DFT calculations that the calculated barrier should be much lower than the above value, roughly on the order of 0.1 kJ/mol or less: Wakamatsu, K.; Toyota, S. Unpublished work.
- (208) Lin, V. S.-Y.; Therien, M. J. *Chem.—Eur. J.* **1995**, *1*, 645.
- (209) Winters, M. U.; Kämratt, J.; Eng, M.; Wilson, C. J.; Anderson, H. L.; Albinsson, B. *J. Phys. Chem.* **2007**, *111*, 7192.
- (210) Kuimova, M. K.; Balaz, M.; Anderson, H. L.; Ogilby, P. R. *J. Am. Chem. Soc.* **2009**, *131*, 7948.
- (211) Bothner-By, A. A.; Dadok, J.; Johnson, T. E.; Lindsey, J. S. *J. Phys. Chem.* **1996**, *100*, 17551.
- (212) Holten, D.; Bocian, D. F.; Lindsey, J. S. *Acc. Chem. Res.* **2002**, *35*, 57.
- (213) Andréasson, J.; Kajanus, J.; Mårtensson, J.; Albinsson, B. *J. Am. Chem. Soc.* **2000**, *122*, 9844.
- (214) Kyrchenko, A.; Albinsson, B. *Chem. Phys. Rev.* **2002**, *366*, 291.
- (215) Shirai, Y.; Osgood, A. J.; Zhao, Y.; Yao, Y.; Saudan, L.; Yang, H.; Yu-Hung, C.; Alemany, L. B.; Sasaki, T.; Morin, J. F.; Guerrero, J. M.; Kelly, K. F.; Tour, J. M. *J. Am. Chem. Soc.* **2006**, *128*, 4854.
- (216) Joachim, C.; Tang, H.; Moresco, F.; Rapenne, G.; Meyer, G. *Nanotechnology* **2002**, *13*, 330.
- (217) Rappene, G.; Jimenez-Bueno, G. *Tetrahedron* **2007**, *63*, 7018.

- (218) Grill, L.; Rieder, K.-H.; Moresco, F.; Rapenne, G.; Stojkovic, S.; Bouju, X.; Joachim, C. *Nature Nanotechnol.* **2007**, *2*, 95.
- (219) Shirai, Y.; Morin, J.-F.; Sasaki, T.; Guerrero, J. M.; Tour, J. M. *Chem. Soc. Rev.* **2006**, *35*, 1043.
- (220) Vives, G.; Tour, J. M. *Acc. Chem. Res.* **2009**, *42*, 473.
- (221) Shirai, Y.; Osgood, A. J.; Zhao, Y.; Kelly, K. F.; Tour, J. M. *Nano Lett.* **2005**, *5*, 2330.
- (222) Sasaki, T.; Osgood, A.; Klappes, J. L.; Kelly, K. F.; Tour, J. M. *Org. Lett.* **2008**, *10*, 1377.
- (223) Sasaki, T.; Osgood, A.; Alemany, L. B.; Kelly, K. F.; Tour, J. M. *Org. Lett.* **2008**, *10*, 229.
- (224) Morin, J.-F.; Shirai, Y.; Tour, J. M. *Org. Lett.* **2006**, *8*, 1713.
- (225) Godoy, J.; Vives, G.; Tour, J. M. *Org. Lett.* **2010**, *12*, 1464.
- (226) Morin, J.-F.; Sasaki, T.; Shirai, Y.; Guerrero, J. M.; Tour, J. M. *J. Org. Chem.* **2007**, *72*, 9481.
- (227) Vives, G.; Kang, J.; Kelly, K. F.; Tour, J. M. *Org. Lett.* **2009**, *11*, 5602.
- (228) Vives, G.; Tour, J. M. *Tetrahedron Lett.* **2009**, *50*, 1427.
- (229) James, D. K.; Tour, J. M. *Top. Curr. Chem.* **2005**, *257*, 33.
- (230) Levitus, M.; Schmieder, K.; Ricks, H.; Shimizu, K. D.; Bunz, U. H. F.; Garcia-Garibay, M. A. *J. Am. Chem. Soc.* **2001**, *123*, 4259.
- (231) Greaves, S. J.; Flynn, E. L.; Fitcher, E. L.; Wrede, E.; Lydon, D. P.; Low, P. J.; Rutter, S. R.; Beeby, A. J. *Phys. Chem. A* **2006**, *110*, 2114.
- (232) Magyar, R. J.; Tretiak, S.; Gao, Y.; Wang, H.-L.; Shreve, A. P. *Chem. Phys. Lett.* **2005**, *401*, 149.
- (233) Hu, W.; Zhu, N.; Tang, W.; Zhao, D. *Org. Lett.* **2008**, *10*, 2669.
- (234) Wyrembak, P. N.; Hamilton, A. D. *J. Am. Chem. Soc.* **2009**, *131*, 4566.
- (235) Nakayama, H.; Kimura, S. *J. Org. Chem.* **2009**, *74*, 3462.
- (236) Thomas, S. W., III; Joly, G. D.; Swagar, T. M. *Chem. Rev.* **2007**, *107*, 1339.
- (237) Swagar, T. M. *Acc. Chem. Res.* **2008**, *41*, 1181.
- (238) Swager, T. M. In Reference 23, Chapter 6.
- (239) Segura, J. L.; Martin, N. *J. Mater. Chem.* **2000**, *10*, 2403.
- (240) Jiang, L.; Gao, J.; Wang, E.; Li, H.; Wang, Z.; Hu, W.; Jiang, L. *Adv. Mater.* **2008**, *20*, 2735.
- (241) Dell'Aquila, A.; Marinelli, F.; Tey, J.; Keg, P.; Lam, Y.-M.; Kapitanchuk, O. L.; Mastrorilli, P.; Nobile, C. F.; Cosma, P.; Marchenko, A.; Fichou, D.; Mhaisalkar, S. G.; Suranna, G. P.; Torsi, L. *J. Mater. Chem.* **2008**, *18*, 786.
- (242) Kaneko, T.; Onuma, A.; Ito, H.; Teraguchi, M.; Aoki, T. *Polyhedron* **2005**, *24*, 2544.
- (243) Kaneko, T.; Makino, T.; Miyaji, H.; Teraguchi, M.; Aoki, T.; Miyasaka, M.; Nishide, H. *J. Am. Chem. Soc.* **2003**, *125*, 3554.
- (244) Rodríguez, J. G.; Tejedor, J. L. *J. Org. Chem.* **2002**, *67*, 7631.
- (245) Rodríguez, J. G.; Tejedor, J. L. *Tetrahedron* **2005**, *61*, 3033.
- (246) Taylor, P. N.; Huuskonen, J.; Rumbles, G.; Aplin, R. T.; Williams, E.; Anderson, H. L. *Chem. Commun.* **1998**, 909.
- (247) Stahl, J.; Bohling, J. C.; Peters, T. B.; de Quadras, L.; Gladysz, J. A. *Pure Appl. Chem.* **2008**, *80*, 459.
- (248) Owen, G. R.; Stahl, J.; Hampel, F.; Gladysz, J. A. *Chem.—Eur. J.* **2008**, *14*, 73.
- (249) Jones, C. S.; O'Conner, M. J.; Haley, M. M. In Reference 23, Chapter 8.
- (250) Spitler, E. L.; Johnson, C. A., II; Haley, M. M. *Chem. Rev.* **2006**, *106*, 5344.
- (251) Wan, W. B.; Brand, S. C.; Pak, J. J.; Haley, M. M. *Chem.—Eur. J.* **2000**, *6*, 2044.
- (252) Marsden, J. A.; Miller, J. J.; Shirtcliff, L. D.; Haley, M. M. *J. Am. Chem. Soc.* **2005**, *127*, 2464.
- (253) Yoshimura, T.; Inaba, A.; Sonoda, M.; Tahara, K.; Tobe, Y.; Williams, R. V. *Org. Lett.* **2006**, *8*, 2933.
- (254) Kissel, P.; Schlüter, A. D.; Sakamoto, J. *Chem.—Eur. J.* **2009**, *15*, 8955.
- (255) Morisaki, Y.; Murakami, T.; Chujo, Y. *Macromolecules* **2008**, *41*, 5960.
- (256) Pu, L. In Reference 23, Chapter 11.
- (257) Ma, L.; Hu, Q.-S.; Musick, K. Y.; Vitharana, D.; Wu, C.; Kwan, C. M. S.; Pu, L. *Macromolecules* **1996**, *29*, 5083.
- (258) Newkome, G. R.; Moorefield, C. N.; Vögtle, F. *Dendrimers and Dendrons*; Wiley-VCH: Weinheim, 2001; p 268.
- (259) Moon, K.-S.; Lee, E.; Lee, M. *Chem. Commun.* **2008**, 3061.
- (260) Moore, J. S. *Acc. Chem. Res.* **1997**, *30*, 402.
- (261) Xu, Z.; Moore, J. S. *Angew. Chem., Int. Ed. Engl.* **1993**, *32*, 246.
- (262) Xu, Z.; Moore, J. S. *Angew. Chem., Int. Ed. Engl.* **1993**, *32*, 1354.
- (263) Jian, H.; Tour, J. M. *J. Org. Chem.* **2003**, *68*, 5091.
- (264) Glass, T. E. *J. Am. Chem. Soc.* **2000**, *122*, 4522.
- (265) Raker, J.; Glass, T. E. *J. Org. Chem.* **2001**, *66*, 6505.
- (266) Raker, J.; Glass, T. E. *J. Org. Chem.* **2002**, *67*, 6113.
- (267) Kelly, T. R. *Acc. Chem. Res.* **2001**, *34*, 514.
- (268) Kelly, T. R.; Bowyer, M. C.; Bhaskar, K. V.; Bebbington, D.; Garcia, A.; Lang, F.; Kim, M. H.; Jette, M. P. *J. Am. Chem. Soc.* **1994**, *116*, 3657.
- (269) Wright, A. T.; Zhong, Z.; Anslyn, E. V. *Angew. Chem., Int. Ed.* **2005**, *44*, 5679.
- (270) Gunderson, V. L.; Mickley Conron, S. M.; Wasielewski, M. R. *Chem. Commun.* **2010**, 401.
- (271) Rein, R.; Gross, M.; Solladié, N. *Chem. Commun.* **2004**, 1992.
- (272) Flamigni, L.; Talarico, A. M.; Ventura, B.; Rein, R.; Solladié, N. *Chem.—Eur. J.* **2006**, *12*, 701.
- (273) Miki, K.; Fujita, M.; Inoue, Y.; Senda, Y.; Kowada, T.; Ohe, K. J. *Org. Chem.* **2010**, *75*, 3537.
- (274) Nandy, R.; Sankararaman, S. *Org. Biomol. Chem.* **2010**, *8*, 2260.
- (275) Godoy, J.; Vives, G.; Tour, J. M. *Org. Lett.* **2010**, *12*, 1464.

CR1000628